TOPICAL REVIEW

Gas–solid interface charge tailoring techniques: what we grasped and where to go

To cite this article: Zhousheng Zhang *et al* 2021 *Nanotechnology* **32** 122001

IOP Publishing Nanotechnology
Nanotechnology 32 (2021) 122001 (32pp) https://doi.org/10.1088/1361-6528/abccea

Topical Review

Gas–solid interface charge tailoring techniques: what we grasped and where to go

Zhousheng Zhang[1], Zheming Wang[1], Gilbert Teyssedre[2], Tohid Shahsavarian[3], Mohamadreza Arab Baferani[3], Geng Chen[4], Chuanjie Lin[5], Bo Zhang[6], Uwe Riechert[7], Zhipeng Lei[8], Yang Cao[3,*] and Chuanyang Li[3,*]

[1] School of Electrical Engineering, Shanghai University of Electric Power, Changyang Road #2588, Shanghai, 200090, People's Republic of China
[2] Laplace, Paul Sabatier University, and CNRS, Toulouse, France
[3] Electrical Insulation Research Center, Institute of Materials Science, Electrical and Computer Engineering, University of Connecticut, Storrs, CT 06269, United States of America
[4] Beijing Area Major Laboratory of High Voltage and Electromagnetic Compatibility, North China Electric Power University, Beijing, 102206, People's Republic of China
[5] State Key Laboratory of Power Systems, Department of Electrical Engineering, Tsinghua University, Beijing, 100084, People's Republic of China
[6] State Key Laboratory of Electrical Insulation and Power Equipment, Xi'an Jiaotong University, Xi'an, 710049, People's Republic of China
[7] ABB Switzerland Ltd, High Voltage Products, Zurich, Switzerland
[8] Shanxi Key Laboratory of Mining Electrical Equipment and Intelligent Control, College of Electrical and Power Engineering, Taiyuan University of Technology, Taiyuan, 030024, People's Republic of China

E-mail: yang.cao@uconn.edu and lichuanyangsuper@163.com

Received 11 June 2020, revised 11 September 2020
Accepted for publication 23 November 2020
Published 30 December 2020

Abstract

Charging of insulators modifies local electric field distribution and increases potential threat to the safety of the gas insulated equipment. In this paper, surface charge tailoring techniques are classified and reviewed by introducing a Dam-flood model. Technical solutions of different charge tailoring methods are compared and discussed. The outlook of potential solutions to suppress charge accumulation is recommended and discussed based on industrial consideration. This paper serves as a guide handbook for engineers and researchers into the study of charge tailoring methods. Meanwhile, we hope that the content of this paper could shed some lights upon charge-free insulators to promote the industrial application of HVDC GIL/GIS.

Keywords: surface charge, fluorination, dielectrics, surface flashover, GIL, charge transport, material modification

(Some figures may appear in colour only in the online journal)

1. Introduction

Surface charge accumulation at the surface of insulators inside the HVDC GIL results in electric field distortion and

* Authors to whom any correspondence should be addressed.

potentially triggers the surface flashover [1]. The pioneering research dates back to 1982 when Cooke found that the insulator surface accumulates charges when the surface charge arrival rate exceeds the surface charge conduction rate [2]. Since then, studies regarding gas–solid interface charge behaviors and characterization techniques [3] as well as charge tailoring methods begin to draw worldwide attentions. Efforts have been paid to control these charges, in which the implementation of nano coatings and fillers played very important role in dielectric property enhancement [4–10].

Nanodielectrics attract more attentions in recent years. The DC conductivity of polyaniline was found increased by doping with TiO_2 nano-fillers, and a very large dielectric constant of about 3700 at room temperature was observed [4]. According to literature 5, a consistency between predictions and impedance measurements verifies the impact of atomic coordination-number imperfection on the dielectric performance of nanometric semiconductors. The effectiveness of nano-fillers is also verified in literature 7 and 8 that a decrease in surface charge accumulation and an increase in surface flashover voltage were obtained. Results from literature 9 again verified that an ordered and nonlinear nano coating introduced on epoxy surface serves as a useful way to decay surface charges and increase surface flashover voltage. A surface treatment creating a nano surface layer by DBD plasma also decays surface charge effectively when using silicone rubber as a base material [10].

In recent years, due to the urgent requirement of HVDC GIL driven by the expansion of HVDC projects, especially offshore projects, the problem of surface charge accumulation has become tremendously pronounced [11–14]. As a consequence, extensive research studies regarding surface charge behavior has become a focus which is a specific challenge [7–10]. However, suitable surface charge tailoring methods still remain to be a difficult problem which captures the interests of researchers.

It has been accepted that the surface charge is either from the conducting current from the volume/surface, or due to charge transport along the direction of electric field lines in the gas phase [15]. Meanwhile, it has been indicated that due to the differences in local electric field stress, dominant charge types at different positions of the insulator are field-dependent, as shown in figure 1 [16]. Surface flashover at DC voltage has been verified to be triggered by expansion of analogous ineffective region due to homo-polar charge injection [17]. Recent study verifies that the evolution of surface charge clusters, presented by dust phase transition, plays a key role in triggering unpredictable insulation surface flashover [14]. Accordingly, when dealing with methods to suppress the surface charge accumulation, it is very important to firstly clarify the dominant charge origin and charge property, as well as the way these charges influence surface flashover voltage under specific insulation-electrode arrangement. Bearing in mind this we can further consider suitable manners targeting the decay of these charges.

In this paper, to help the reader identify the source of the charge at the gas–solid interface, which is very important while usually be neglected, and the suppression methods more intuitively, we introduce a Dam model to explain

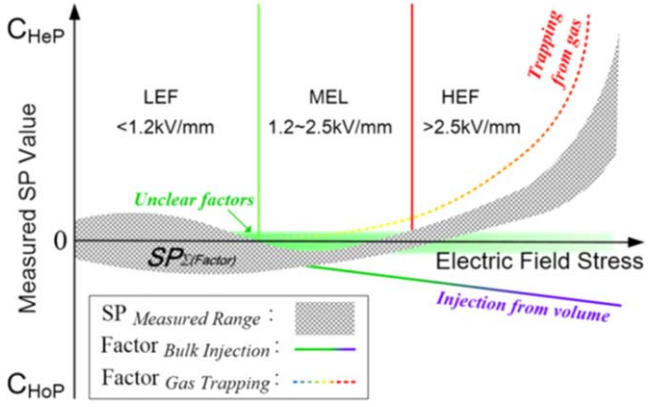

Figure 1. Field-dependent model of dominant charge behavior. Unclear factors represents electrostatic charges, bulk charges, charges from cosmic or PDs, and polarization in the volume, etc; trapping from gas represents enhanced gas ionization following Townsend's law; injection from volume represents charges injected from volume; SP, $C_{He}P$, and $C_{Ho}P$ stand for surface potential, hetero-polar charge and homo-polar charge. Reprinted from [16], with the permission of AIP Publishing.

interestingly how gas–solid interface charges are categorized based on which the corresponding charge tailoring methods are reviewed and discussed. The outlook of potential solutions to suppress charge accumulation is recommended and discussed based on industrial consideration. We hope that this paper can be useful for engineers and researchers into the study of charge modification methods and could shed some lights upon charge-free insulators to promote the industrial application of HVDC GIL/GIS.

2. Dam-flood model

Causing heavy casualties, the flood to houses and populations is equivalent to the charge triggered surface flashover to gas insulated electric power systems. The triggering process for floods can be slow which is due to the destruction/degradation of the forest over years, while some types of floods can be developed over a few days due to continuous heavy rain drop. Correspondingly, surface charge accumulation on the insulator can be a very slow process due to numerous discrete processes on smallest scale, e.g. charge injection/extraction at the electrode-insulation interfaces, trapping and de-trapping, charge generation and recombination, polarization, etc [18], while in some cases the surface charge amount can be increased dramatically in a short period in case of ionization due to local metal particles [2].

The dam, representing as the insulator to separate high voltage from the ground, is a barrier that restricts or stops the flow of water and suppresses progression of the floods. The solution for flood control via the construction of a dam can be divided into four aspects: *Flood spilling*, *dam strengthening*, *dredging* and *comprehensive management*, which corresponds to different charge tailoring orientations, as shown in table 1 and figure 2. To be more specific, in case when the upstream water level rises, spilling prevents flooding in a

Table 1. Flood-dam model and the corresponding surface charge tailoring techniques.

Flood-dam model	Corresponding orientation for charge suppression	Key points	Features	Literature
Flood-spilling	Increasing surface charge decay	Direct fluorination	Increasing surface charge decay rate by increasing surface conductivity	[19–37]
		Etching; deposition		[38–45]
		SiO_2/Epoxy coating; TiO_2/Epoxy coating		[46, 47]
		Gamma rays; ozone treatment; radical scavenger		[48–51]
Dam reinforcement	Inhibiting homo-polar charges from volume	Cr_2O_3 coating	Suppressing charge injection at metal-dielectric interface by introducing deep traps	[34, 52]
		$K_2Ti_6O_{13}$ Whisker; C_{60} particle	Suppressing conducting current	[53, 54]
Dredging	Decaying/avoiding charges near high electric field zone	Shape modification	Optimizing local electric field	[2, 55–63]
		Nonlinear particles; non-linear coatings	Optimizing local electric field and increasing local surface charge dissipation	[9, 64–72]
Comprehensive management	Initiatively controlling and decaying charges	Modifying spacer shape and doping with nonlinear materials	Adaptively controlling the charge location and decay property	[73–76]

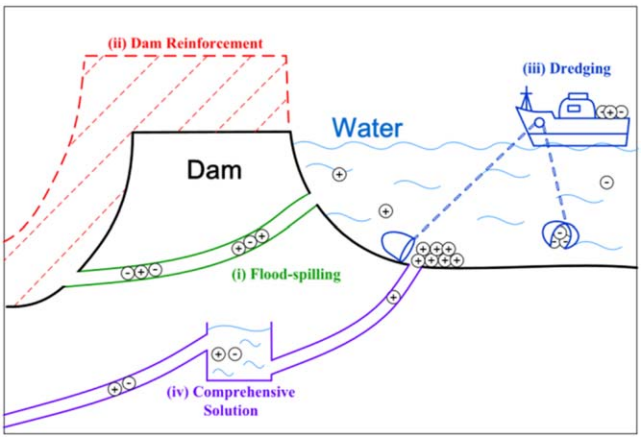

Figure 2. Equivalent diagram of Dam-flood model.

manner of keeping water flowing downstream, which is equivalent to increase the surface charge decay rate to have a lower amount of surface charges; by *dam reinforcement*, the dam becomes stronger so that the water pressure does not endanger the safety of the dam, which is equivalent to increasing the inception electric field for charge injection so as to suppress injected homo-polar charges; *Dredging* is a commonly used approach to increase the canal depth and therefore increase the capacity of canals for carrying water/floods. Regarding the charge tailoring solution, by means of material modification and shape improvement, local electric field can be optimized and the withstand voltage of the spacer can thereby be increased; Based on canal diversion, the sediments can be dredged and saved for farmlands and the flood can be prevented. Such *comprehensive management* methods have the synergistic effect to control surface charges of insulators, i.e. to control the position of charges and initiatively decay these charges. The Dam model constituents and the corresponding surface charge tailoring techniques can also be found in table 1.

3. Flood-spilling-increasing surface charge decay

Given the idea of *Flood spilling*, a more conductive surface with higher surface decay rate is obtained. Capability of fluorination, plasma treatment, surface coatings, gamma ray irradiation, and ozone treatment, etc, have been verified in increasing the surface conductivity and surface charge decay by researchers [31, 34, 38, 46, 48, 50]. This chapter firstly reviews the results from the above mentioned methods, and a comparative analysis among the research characteristics from each research group is presented.

3.1. Surface fluorination

Surface fluorination treatment is performed based on the interaction between fluorine gas and the polymer surface. A stable C-F surface layer with different byproducts can be formed and thereby the surface property can be controlled

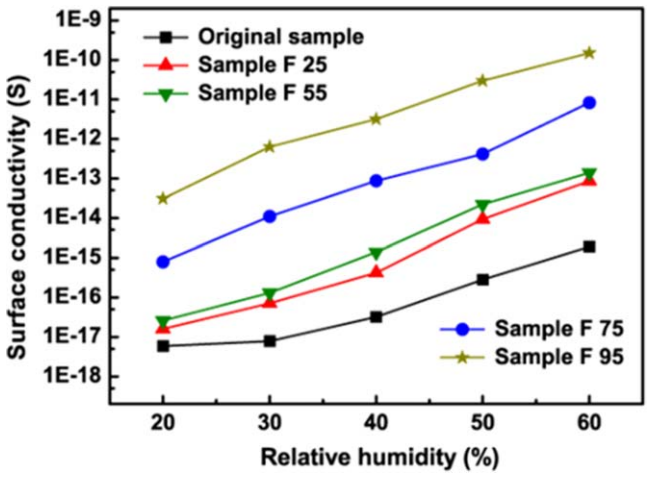

Figure 3. Surface conductivity measured at different RH levels and room temperature for the original sample and samples fluorinated at 25 °C, 55 °C, 75 °C, and 95 °C. © 2013 IEEE. Reprinted, with permission, from [22].

[25] and a fluorinated coating with certain surface conductivity is obtained.

3.1.1. Researches in Tongji University. In 2011, An *et al* conducted pioneering researches on surface fluorination treatments on epoxy resin [21]. They used an F_2/N_2 mixture with a volume of 12.5% F_2 to fluorinate the epoxy resin sheet with a thickness of 0.55 mm, and the results showed that the surface conductivity was increased from 1.1×10^{-17} to 8.7×10^{-14} S, with a value increasing by 3 orders of magnitude. They believed that the decrease of surface trap depth and the adsorption of water on the surface in the vicinity of air are the main reasons responsible for increase of surface conductivity. Based on their preliminary results, they modified epoxy sheet to suppress the accumulation of surface charges effectively by introducing a surface with lower conductivity through the fluorination [20]. In order to further understand the mechanism of the suppression of the charge accumulation on the insulator surface, they further studied the effect of temperature and fluorination duration on electrical properties of epoxy based materials [22].

Figure 3 shows the surface conductivities of the epoxy before and after fluorination. The results showed that the surface conductivity of the fluorinated sample at various humidity levels is significantly higher than the untreated sample, and the surface conductivity increases with the increase of the fluorination temperature. They concluded that the increase in fluorination temperature increases surface conductivity (from 10^{-17} to 10^{-13} S at 20% relative humidity level).

Further, they showed that the surface conductivity of samples can be related to fluorination time duration at different relative humidity levels [23]. Figure 4 shows the surface conductivity of the original and surface fluorinated samples at different relative humidity levels. The results show that as the fluorination time duration increases, the surface

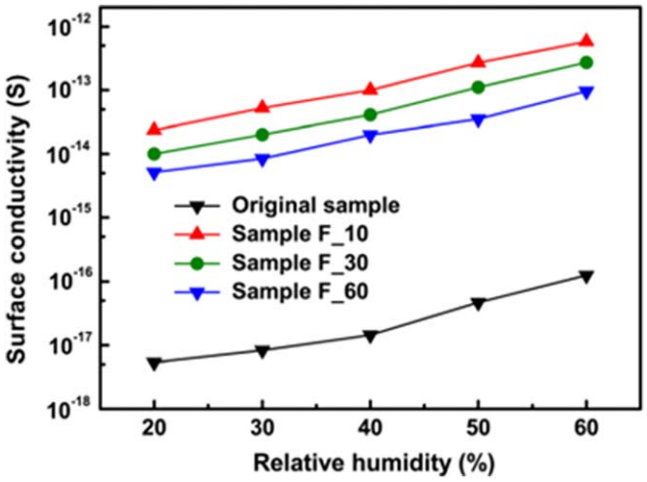

Figure 4. Surface conductivity at different RH levels for the untreated and surface fluorinated samples for times of 10, 20 and 30 min. Reprinted from [23], with the permission of AIP Publishing.

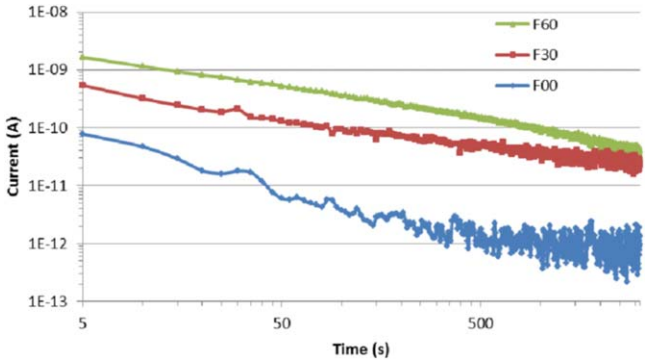

Figure 5. DC conductivity measurement for 250 μm epoxy resin sample being treated after different fluorination time. © 2014 IEEE. Reprinted, with permission, from [30].

conductivity increases, while this trend is opposite in case of humidity changes.

They concluded that temperature and fluorination time duration are two important factors controlling the fluorination process and the surface conductivity, noting that the effect of temperature on the surface conductivity is more significant than that of the fluorination time duration [19]. In subsequent researches, they investigated the discharge characteristics and AC/DC flashover performance of surface fluorinated epoxy insulators [24, 37].

3.1.2. Researches in university of Southampton. Chen *et al* employed the same fluorination treatment method on the epoxy films [28–30]. Compared with An's work, Chen's research paid more attention on the breakdown property of the epoxy. They found that with the prolongation of the fluorination time duration, the surface flashover voltage was increased significantly. Meanwhile, their results showed that the leakage current increases with the fluorination duration, which is different compared with results obtained by other researchers [20–22, 33]. As shown in figure 5, the leakage current of samples fluorinated for 30 min and 60 min are

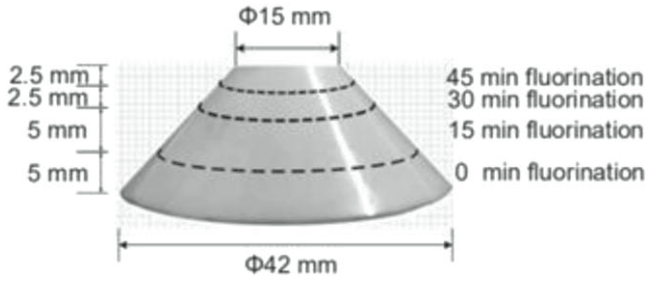

Figure 6. Insulators with interfacial σ-FGM: a four-gradient tapered insulator (F-45-30-15-0). © 2019 IEEE. Reprinted, with permission, from [32].

2.4×10^{-11} A and 4.12×10^{-11} A, respectively, which is much higher than that of the untreated sample.

In their subsequent studies, they paid more attention to the charge suppressing mechanism [26]. They believed that the increase in the surface conductivity may not be due to the fluorine layer itself, but because of the moisture absorbed by the surface layer [27]. It is interesting to note that according to a recent report, the conductivity of the fluorinated layer has a negative correlation with increase of the temperature [15], while the result provided by Chen implies that increase of the conductivity by fluorination process is due to absorbed surface moisture, which can be the rationale behind this phenomenon.

3.1.3. Researches in Tianjin university. Du *et al* Studied the surface charge decay property of fluorinated epoxy samples [31]. The surface flashover voltage of samples with different fluorination time durations are evaluated. They introduced the carrier mobility and trap distributions to analyze the effect of fluorination on surface charge behaviors and flashover characteristics [31]. Furthermore, a novel cone-type insulator with surface conductivity gradient based on direct fluorination treatment was developed, as shown in figure 6 [32]. The results showed that the flashover voltage of the σ-FGM insulator is 36.3% higher than that of the traditional insulator due to a uniform electric field distribution.

3.1.4. Researches in Tsinghua university. Following An 's pioneering research regarding fluorination of epoxy resin, He *et al* focused mainly on surface fluorination treatment of Al_2O_3 filled epoxy resin insulators, which pushed these researches much closer to the industry applications [25]. In their studies, different surface modification methods are employed to evaluate the effect of fluorination on epoxy based insulation products [33, 34, 36],

Electroluminescence as a parameter to characterize epoxy-based composites before and after fluorination was introduced [35]. Here electroluminescence is defined as a surface light emission that may involve both solid and gas emissions following impact by energetic carriers. It has to be distinguished from pure bulk emission from solids that normally require higher fields to be triggered [77, 78]. The results showed that the electroluminescence curve of the sample after fluorination is more stable than that of the non-fluorinated sample (as shown in figure 7), and the EL pulse

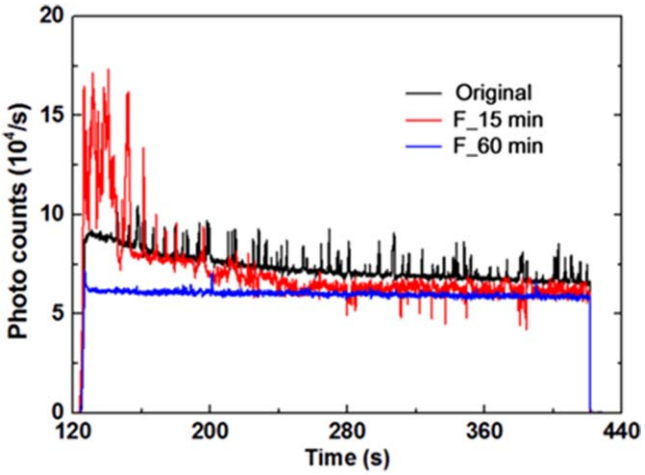

Figure 7. Electroluminescence intensity of samples before and after surface fluorination at −20 kV. Reproduced from [35]. CC BY 4.0.

corresponding to the F_60 min sample is significantly suppressed. They believed that the surface of the sample becomes flatter after fluorination, thereby the micro plasma activities due to the concentration of the electric field on the surface alumina edges and corners at the gas–solid-conductor triple junction are suppressed. They emphasized that these micro-discharges are likely to be a potential consequence of surface heteropolar charges and can thereby increase the possibility of undetermined surface flashover under both AC and DC voltage, which were also discussed in their follow-up research work [14, 79]. In 2017, the physical mechanism of fluorination on carrier migration and the impact on flashover voltage were explored and the inhibitory effect of fluorination on surface discharge corrosion was preliminary studied (as shown in figure 8(a)) [36]. An further studied the improvement of surface electro-corrosion performance by fluorination in 2019 [24] (as shown in figure 8(b)). Both researches confirmed the resistivity of the fluorinated epoxy surface layer to corona discharge is significantly improved [24, 36].

3.1.5. Analysis and discussion. Looking at the similarities of the results in these 4 different groups, we can conclude that several key parameters play important roles in determining surface properties, among which the surface conductivity, trap distribution, surface morphology significantly affect the surface charge decay and surface flashover voltage. However, based on the results of previously published literature, it is still difficult to confirm which parameter plays dominant role on surface charge decay process and surface flashover property. Table 2 shows the surface conductivity values presented in different research studies. Two general conclusions can be obtained: (1) The surface conductivity is increased dramatically with short fluorination time (within 30 min), while it decreased when the samples are treated after long term fluorination, except for results obtained by Chen [28, 29]. (2) The decreasing rate of conductivity with fluorination time duration accelerates with increase of temperatures. Apart from that, based on the results presented in [22, 23, 25, 33], the surface conductivity of untreated epoxy or epoxy based composites ranges from 9×10^{-22} to 7×10^{-18} S, with the difference up to 1–4 orders of magnitude in their values. Usually, the leakage current has very large difference with respect to electric field, temperature and duration of applied dc voltage. Meanwhile, if the measurement was repeated for several times, the injected charges and depolarization process from previous tests can further influence the leakage current, resulting in a lower leakage current value. When it comes to samples after fluorination, we can find some similarity that the surface conductivity can be increased by 3–5 orders of magnitude with short fluorination time, while the long fluorination time results in a surface with conductivity similar to the untreated samples. This finding is applicable to both alumina-doped epoxy and pure epoxy.

It has been widely accepted that a higher surface conductivity results in a higher surface charge decay rate. However, it should be pointed out that the increase in surface flashover voltage due to fluorination cannot merely be attributed to increase of charge decay kinetics. In [33], the surface conductivity of fluorinated sample for 60 min is 8.64×10^{-19} S, which is slightly lower than the surface conductivity of untreated samples 8.92×10^{-19} S (refer to table 2), while the flashover voltage, similar to that with short fluorination time, is much higher than the untreated sample (as shown in figure 9). We believe that the surface morphology after long fluorination time has more influence on surface flashover voltage than the surface charge decay.

Considering the feasibility of industrial applications, fluorination is applicable to insulators of any shape and size. However, it has disadvantages such as: the mechanism of the fluorination is complex, which needs further investigation. In addition, it is still unclear that the fluorinated coating can be stable since insulators are exposed to temperature variation under dc voltage. As for the aging of the fluorination layer, Shao tested the surface charge decay rate using sheet samples, and the results showed that there is no obvious aging effect after 5 d storage of the directly fluorinated samples in ambient air [42]. However, the experiment was conducted in the ambient air, which cannot demonstrate real operation condition subjected to temperature and electric field changes, so it cannot be regarded as a direct fluorination stability test.

As reported in our recently published paper, the conductivity of the fluorinated layer has a negative correlation with the increase of temperature (as shown in figure 10). This means that when the temperature rises, the conductivity of the fluorinated layer decreases, which can reduce the rate of charge dissipation [15]. This process has been verified, which is not reversible. In this case, the surface charge decay rate for short time fluorianted spacer would somehow be affected.

3.2. Plasma treatment

Plasma refers to an ionized gaseous medium which consists of a gas of ions and free electrons. Based on its unique property, it can be used to modify dielectric surface, modifying surface trap level distribution, carrier mobility, and surface conductivity of the material [38, 39, 41, 42]. Commonly used low-temperature plasma-treated discharge includes dielectric

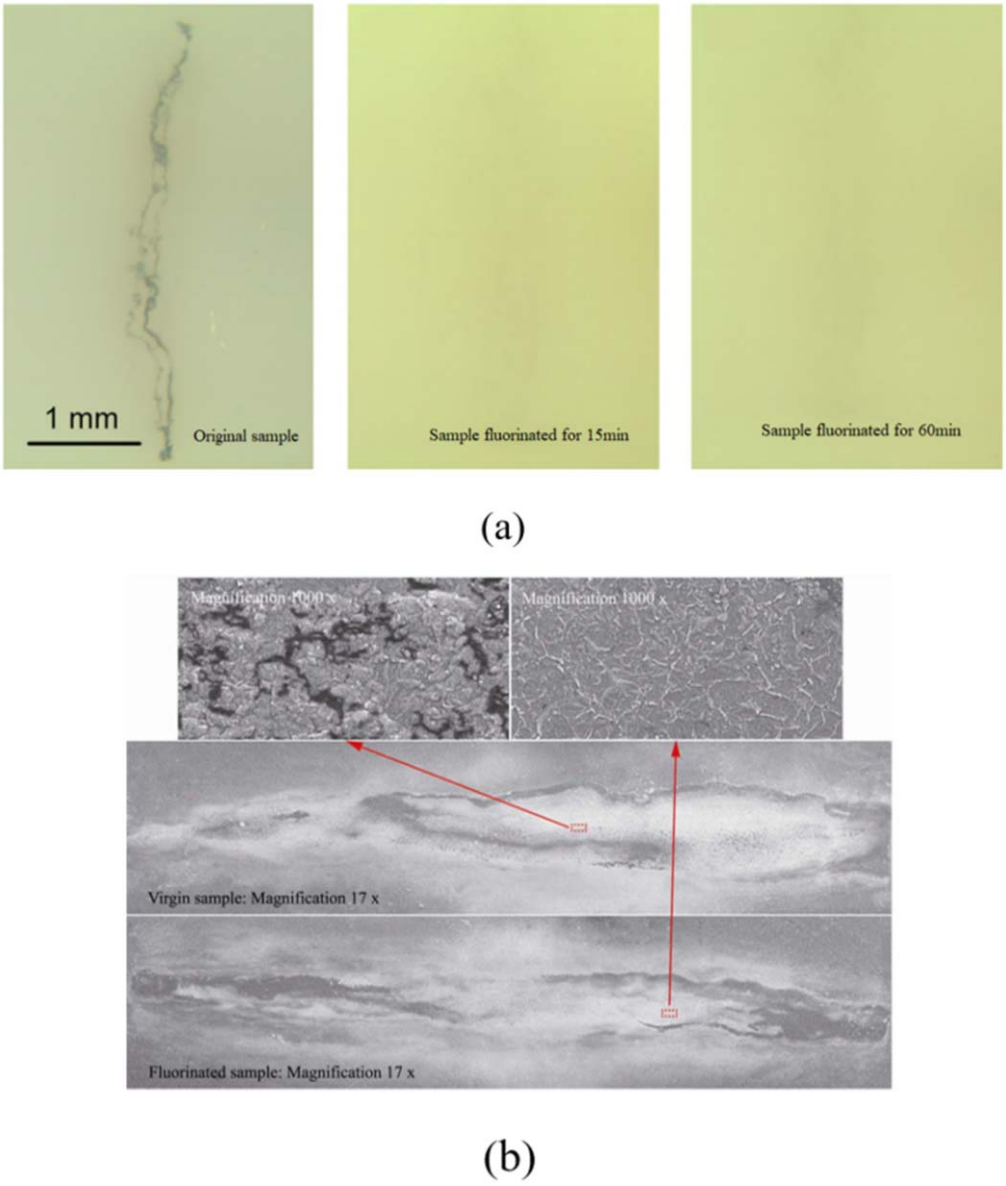

Figure 8. (a) Surface image of experimental samples before and surface flashover in SF_6. Reproduced from [36]. © IOP Publishing Ltd. All rights reserved; (b) SEM photographs of the discharge degraded surface of the virgin and the fluorinated samples respectively after the 5th and 10th flashover. © 2018 IEEE. Reprinted, with permission, from [24].

barrier discharge (DBD), atmospheric pressure plasma jet (APPJ), and the like. In this section, we focus on studies regarding plasma-treated surface and the dielectric property enhancement.

3.2.1. Researches in Chinese academy of sciences. Electrons in non-thermal plasmas can induce molecule excitation, ionization and dissociation, hence, resulting in the chemical bonds breaking for surface modification [80, 81]. Shao *et al* performed pioneering studies over DBD plasma treatment in epoxy based polymers and found that the plasma treatment effectively increases the surface hydrophilicity of epoxy resin, which in turn augments surface charge decay rate [39]. Meanwhile, the anti-aging property of the epoxy-based samples was studied. Figure 11 shows the surface potential decay of samples after the plasma treatment. Samples were charged by corona discharges with a amplitude of −4.5 kV, the temperature was 20 °C and the relative humidity was 20%. The results showed that the surface potential decay was slower on the samples measured after 4 days, while the aging resistance of the atmospheric-pressure dielectric barrier discharge (AP-DBD) etching method is not improved significantly.

Based on their previous research results, they further conducted in-depth research on sample modification methods based on plasma treatment in 2017 [40, 41, 44]. They found out that the plasma deposition process can increase the aging resistance more effective than the direct plasma treatment mentioned in their previous work [39]. In their test setup, non-thermal plasma generated by gliding arc discharge driven by high-frequency high-voltage power supply are used to deposit SiO_2 film on the surface of epoxy resin, and the reaction precursor is tetraethyl orthosilicate (TEOS) [44]. They realized

Table 2. Fluorination test conditions and results of different research groups.

			Surface conductivity test conditions			Fluorination parameter		
Authors	References	Matrix	Ambient gas	Temperature (°C)	Relative humidity	Fluorination temperature (°C)	Fluorination time (min)	Surface conductivity (10^{-18} S)
An	[22]	Epoxy resin	Air	25	20%	—	—	7
						25	30	20
						55		40
						75		900
						95		50 000
	[19]	Epoxy resin	High purity N_2	25	20%	—	—	9
						25	30	10
						55		30 000
						75		300 000
						95		800 000
	[23]	Epoxy resin	Air	25	20%	—	—	7
						50	10	40 000
							30	10 000
							60	8000
Chen	[27]	Epoxy resin	Air	25	Before drying	—	—	1886
						50	60	4940
					After vacuum drying	—	—	1406
						50	60	2040
			N_2	25	After N_2 drying	—	—	1406
						50	60	3480
	[26]	Epoxy resin	Air	25	Not mentioned	—	—	113.2
						50	30	432
							60	1006
Du	[32]	Epoxy/Al_2O_3	Air	25	Under 30%	—	—	450
						25	15	800
							30	1400
							45	1790
							60	1900
He	[25]	Epoxy/Al_2O_3	High purity N_2	25	Under 10%	—	—	0.000 97
						50	15	370
							30	21
							60	0.86
	[33]	Epoxy/Al_2O_3	Air	16	10%–14%	—	—	0.88
						50	15	368
							30	20.5
							60	0.86
	[33]	Epoxy/Al_2O_3	SF_6	16	10%–14%	—	—	0.892
						50	15	374
							30	21
							60	0.864

that when the deposition time exceeded 5 s, a thin film with a thickness of 219 nm containing Si–O–Si and Si–OH groups can be stably formed on the epoxy surface. Meanwhile, with this surface layer, the water contact angle and the surface resistivity were significantly reduced compared with pure epoxy samples, which increases surface charge decay rate significantly [41].

Shao *et al* further studied the feasibility of plasma deposition on surface charge property and deposited SiO_x thin film on the surface of epoxy resin by AP-DBD [38, 40]. The results showed that the initial surface charge density was reduced by 12% and the flashover voltage was increased by 42% after plasma deposition treatment. They believed that the

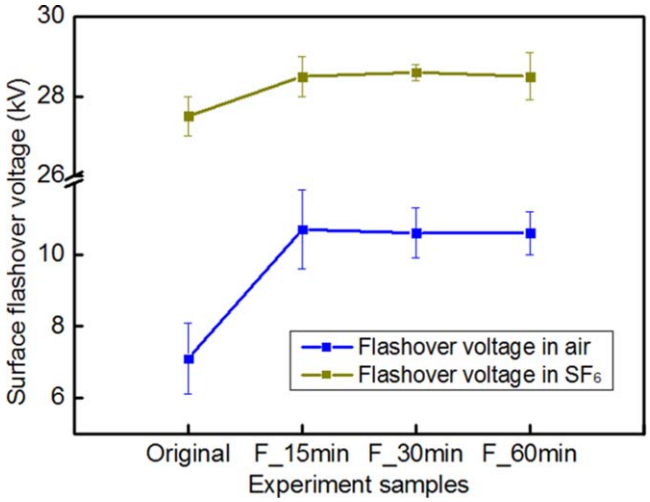

Figure 9. The DC surface flashover voltage of original and fluorinated samples for 15 min, 30 min and 60 min in air and SF_6. © 2016 IEEE. Reprinted, with permission, from [33].

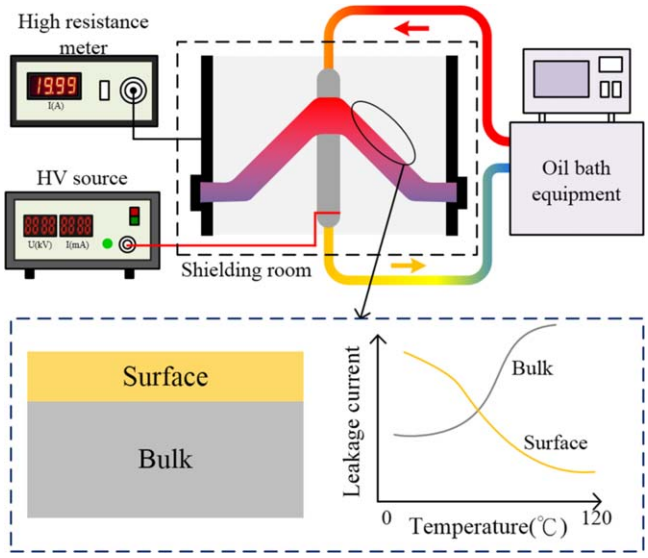

Figure 10. Stable surface leakage current and bulk leakage current changing trend with the increase of temperature using a new short time fluorinated spacer. © 2019 IEEE. Reprinted, with permission, from [15].

mechanism for the increasing of these properties is due to the fact that SiO_x films with a thickness of 50–200 nm introduce shallow traps, which increases the surface conductivity and thereby reduce the accumulation of surface charges. In 2019, they compared the effect of the three methods of plasma etching, plasma deposition and direct fluorination on the basis of previous researches [42, 43]. The surface charge decay rate of epoxy based samples after DBD deposition (96%) and fluorination (95%) is higher than DBD etching (34%) [43]. The results from the above mentioned studies indicate that AP-DBD deposition has best performance in increasing the surface charge decay rate of the sample [42].

3.2.2. Researches in Xi'an Jiaotong university. Min *et al* studied the effect of surface plasma treatment on the surface charge decay property of epoxy based composite with different treatment time (1 min, 3 min, 5 min) [45]. They found out that the surface conductivity reaches 1.4×10^{-17} S which is 2 orders of magnitude higher than that of untreated samples. Meanwhile, the correlation between surface flashover and the surface conductivity showed that the DC surface flashover voltage increases with the increase of the surface conductivity (figure 12), whose reason they believed was due to the surface charge decay [45].

3.2.3. Analysis and discussion. Table 3 shows the key parameters selected for each research group according to different treatment methods. Most of the results show an upward trend regarding the surface conductivity of samples after plasma treatment, with the increasing value of 1–4 orders of magnitude. However, it is worth noting that contrary to changing laws of surface conductivity after fluorination, the surface conductivity after plasma treatment for 1 min is higher than that after treated after 5 min. That is to say that the longer the processing time, the higher the surface conductivity will be. Meanwhile, it should be emphasized that DBD deposition methods showed excellent anti-aging performance than AP-DBD [42, 43]. However, the problem regarding forming a uniform discharge to coat the sample surface of large areas ready for industrial applications should be further studied.

3.3. Coatings

Commonly used coatings to modify surface charge behaviors include: magnetron sputtering coatings, spray coatings, dipping and plasma coatings.

3.3.1. Research review. Nano-TiO_2/EP coatings can increase surface charge decay of epoxy resin, which was developed by Tu *et al* [47]. When the content of nano-TiO_2 particles is 1% and 3%, the surface charge is mainly concentrated near the high-voltage electrode while when the content of nano-TiO_2 particles is 5% and 7%, the surface charge settles near the grounded electrode. When the particle content is 3%, the surface conductivity reaches a maximum value which is 2×10^{-17} S [46].

Meanwhile, Du *et al* prepared epoxy (EP)/graphene (GR) coated insulators with different doping ratios by dipping and found out that the flashover characteristics of the samples are increased dramatically, as shown in figure 13 [82]. However, they verified that when the content of nanographene reaches 0.15%, the flashover voltage of EP/GR coated insulators is lower than that of uncoated insulators. They believed that adding of proper nanographene content on the surface layer increases the trapping energy and density of EP/GR composites; thereby the surface charge decay rate of the insulator is increased.

Zhang *et al* proposed a structurally nacre-mimetic coating on epoxy insulators achieved by using a facile flow-induced co-assembly technique. By doing so, a faster charge dissipation and higher surface flashover voltage were observed, as shown in figure 14 [83].

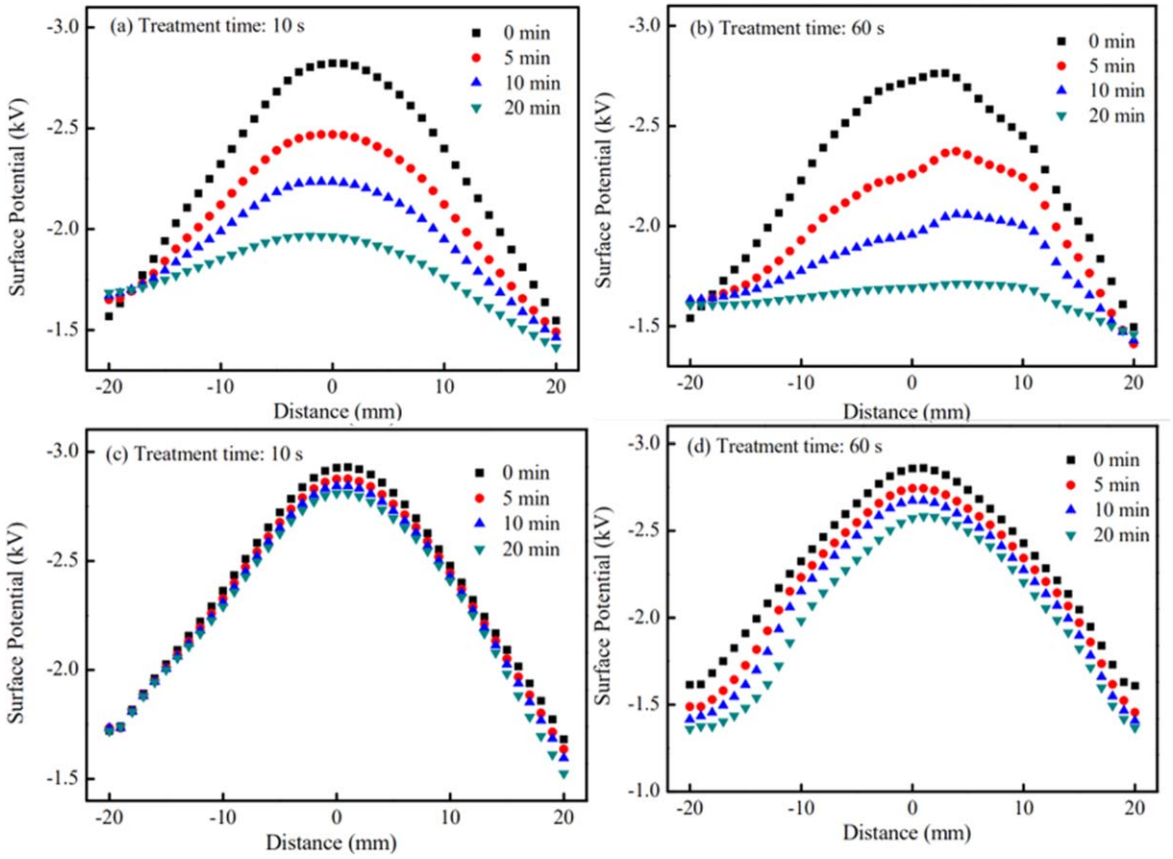

Figure 11. The surface potential decay of epoxy samples aging effect (a) and (b) with plasma treatment time 10 and 60 s measured right after plasma treatment (c) and (d) with plasma treatment time 10 and 60 s measured 4 d later. © 2017 IEEE. Reprinted, with permission, from [39].

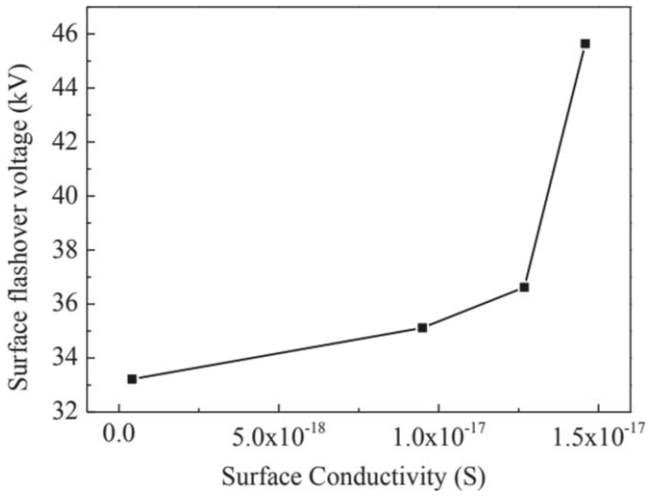

Figure 12. Relation between surface flashover voltage and surface conductivity. © 2018 IEEE. Reprinted, with permission, from [45].

3.3.2. Analysis and discussion. Table 4 summarized the feature parameters regarding epoxy coatings in the above mentioned research groups. In addition to the parameters researches focusing on after fluorination or plasma treatment, i.e. surface conductivity and surface roughness, these two research groups attempt to explain charge tailoring mechanism by introducing the charge carrier mobility. Tu *et al* observed that, the carrier mobilities of the coatings, with 1 wt% and 3 wt% micro-SiO_2 particles, reach as high as 11×10^{-13} and 17.5×10^{-13} $m^2 V^{-1} \cdot s^{-1}$, while the carrier mobility introduced by nano-SiO_2 particle composite coatings with a doping amount of 3 wt% is the highest around 86×10^{-13} $m^2 V^{-1} \cdot s^{-1}$. The above three samples have been verified effectively to inhibit the accumulation of surface charges on epoxy resins. However, in the study conducted by Du *et al* the 0.1 wt% nanographene/EP composite coating results in a DC flashover voltage of up to 33 kV, while the carrier mobility of this sample shows the lowest value around 0.14×10^{-13} m^2 $V^{-1} \cdot s^{-1}$ compared with other samples. However, the carrier mobility of the samples in [46] is 2 orders of magnitude higher than that in [82]. Therefore, it can be assumed that the carrier mobility can only be used as an auxiliary basis for explaining surface flashover voltage, while other factors such as the coating material intrinsic property, surface morphologies, etc need to be comprehensively evaluated. The dominant factors to determine the effectiveness of surface charge controlling methods on insulators need to be further explored. In addition, the anti-aging property of the coating and its stability against the cold and heat cycles still need further consideration, which also greatly limits the industrialization of such coatings methods.

3.4. Other methods

In addition to the methods already mentioned, the following techniques are also discussed by researchers as candidates to

Table 3. Treatment time and results of different plasma processing methods.

Research group	References	Treatment type	Processing time	Surface conductivity (10^{-18} s)
Shao	[44]	Untreated	0	1810
		Plasma enhanced chemical vapor deposition (PECVD) to deposit SiO_2 thin films	1 s	3810
			3 s	6390
			5 s	24 100
			10 s	85 100
			15 s	113 000
	[39]	Untreated	0	30 000
		AP-DBD etching	10 s	68 000
			60 s	190 000
			180 s	250 000
	[38]	Untreated	0	900
		APPJ plasma treatment to deposit SiO_x film	1 min	9000
			3 min	70 000
			5 min	60 000
			10 min	30 000
	[43]	Untreated	0 min	900
		AP-DBD etching	5 min	7000
		AP-DBD plasma treatment to deposit Ar/TEOS	10 min	300 000
		Direct fluorination	30 min (At 50 °C)	90 000
	[42]	Untreated	0	270.3
		AP-DBD plasma treatment to deposit Ar/TEOS	5 min	1000 000
			10 min	1010 000
		Direct fluorination	15 min (At 50 °C)	3330
			30 min (At 50 °C)	50 000
			60 min (At 50 °C)	100 000
	[40]	Untreated	0	2230
		AP-DBD deposited SiO_x film	3 min	2000 000
			5 min	5000 000
			10 min	54 700 000
Min	[45]	Untreated	0	0.1
		HD-1B plasma modification device	1 min	13
			3 min	14.5
			5 min	10

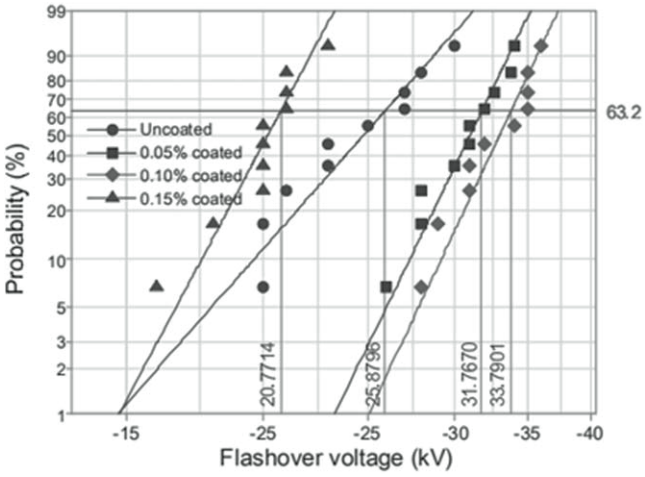

Figure 13. Weibull distributions of flashover voltages of the uncoated and epoxy (EP)/graphene (GR) coated insulators. © 2019 IEEE. Reprinted, with permission, from [82].

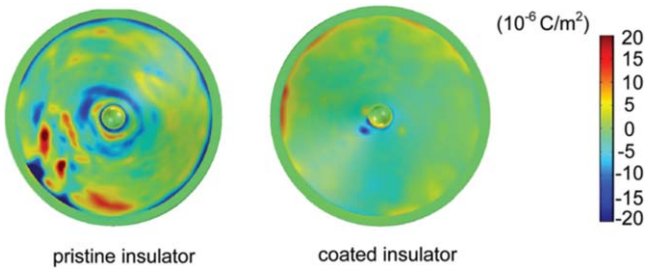

Figure 14. Surface charge density distribution on cone-type insulators after application of a −20 kV dc voltage for 30 min. Reproduced from [83] with permission of The Royal Society of Chemistry.

modify surface charge behaviors, which includes: gamma ray treatment, roughness treatment, ozone treatment, and radical scavenger treatment.

3.4.1. Gamma rays. In 2010, Gao *et al* found that the surface charge decay rate of epoxy insulator is accelerated after epoxy

Table 4. Relationship between carriers and doping amount of different coating materials.

Research group	No./ref	Coating material	The average particle size of the coating doped particles 10^{-9} m	Coating thickness 10^{-6} m	Coating doping content wt%	Carrier mobility 10^{-13} m^2 $V^{-1} \cdot s^{-1}$
Tu	[46]	Nano-SiO_2/EP composite coating	60	170–190	0	7
					1	5.2
					3	86
					5	30
	[46]	Micron SiO_2/EP composite coating	700		1	11
					3	17.5
					5	9.5
Du	[82]	Nanographene/EP composite coating	500–5000	Not mentioned	0	0.38
					0.05	0.18
					0.1	0.14
					0.15	0.46

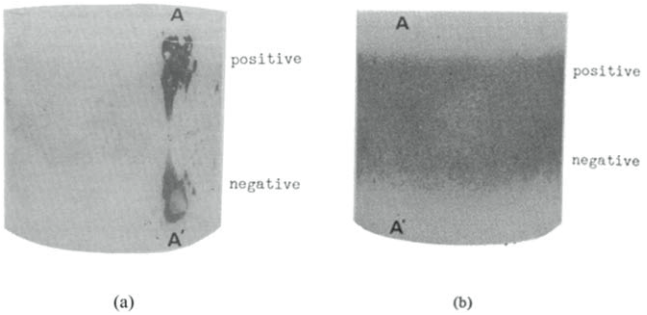

Figure 15. Probe measurement of residual charge distribution on the spacer. (a) The untreated sample, (b) The sanded sample. © 1983 IEEE. Reprinted, with permission, from [59].

sample being treated by gamma rays, and the surface potential decay rate shows the best results when using the 1000 kGy irradiated sample [48, 49]. They attributed the increased charge dissipation to the decrease in trap depth.

3.4.2. Surface roughness treatment. In 1983, Nakaishi *et al* found that unpolished cylindrical insulators present a 'bow-tie' like surface charge distribution under DC voltage (as shown in figure 15), and the surface charge uniformly distributes when the surface is polished, believed to be attributable to the increase in conductivity after grinding [59].

Kumada *et al* conducted similar work to change the surface smoothness of the conical epoxy insulator with sandpaper. They found lower surface charge density in the polished areas, but a large amount of charges accumulate at the junction of the polished and unpolished areas, as shown in figure 16. Based on such findings, they believed that the uneven conduction on the insulator surface is the cause of the surface charge accumulation [84].

Further, Xue *et al* studied the surface charging property and surface flashover characteristics in SF_6/N_2 mixed systems using epoxy alumina insulator samples with different surface roughness [85]. Under positive DC voltage, the average surface flashover voltages for samples with surface roughness of 0.58 μm, 5.19 μm, 7.48 μm, and 9.24 μm were 15.48 kV, 16.24 kV, 16.76 kV, and 17.55 kV, respectively. Compared with the untreated surface (0.58 μm), the positive DC voltage increased by 4.86% (5.19 μm), 8.27% (7.48 μm), and 13.32% (9.24 μm), respectively (as shown in figure 17). The DC flashover voltage can be increased by 20% to 25% after the surface is roughened. They believed that the increase in surface flashover voltage firstly is mainly due to the increase in the leakage distance caused by surface treated roughness and blockage. Secondly, the surface conductivity was decreased slightly, but it was still higher than untreated sample. At the same time, the introduced deep traps would also inhibit the surface charge accumulation, increase the insulation strength, and increase the corresponding flashover voltage. It is concluded that the surface roughness treatment can suppress the surface charge accumulation and improve the surface flashover voltage.

3.4.3. Ozone treatment. The effect of ozone treatment on the surface flashover performance of epoxy/Al_2O_3 composite was studied and the results showed that the surface conductivity by ozone treatment for 4 h is increased by 2 orders of magnitude compared with the untreated sample, as shown in figure 18 [50]. The density of shallow traps increases with the increase of treatment time, while the energy of shallow surface traps decreases with the increase of treatment time. Authors believed that the change in these two parameters simultaneously increases the charge carrier of the sample and increases the surface charge dissipation rate.

3.4.4. Radical scavenger. In 2013, Tarik Baytekin *et al* proposed that scavenging for free radicals from surface could be a more efficient way to increase surface charge decay rate, than controlling the surface charges itself [51]. They argued that these free radicals coexist with the charge and stabilize

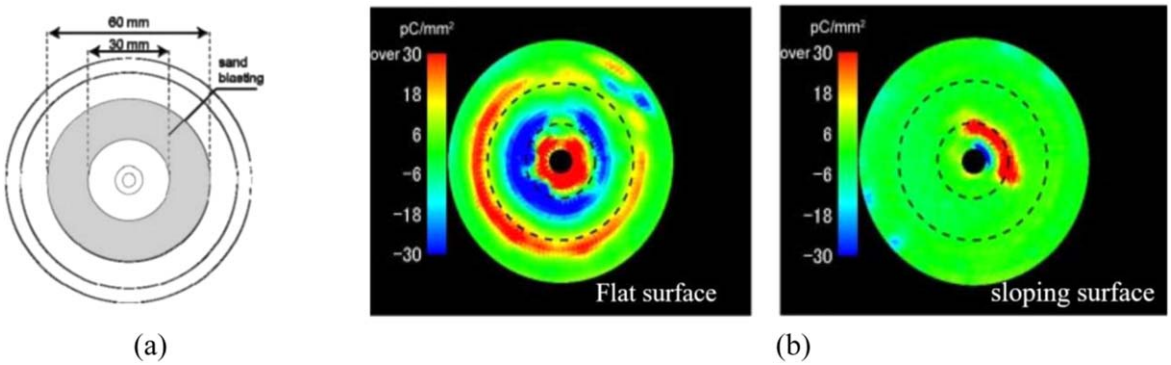

Figure 16. (a) Sand blasted region on the spacer. (b) Charge distribution after 240 h' voltage application for the spacer with nonuniform surface conductivity. [84] John Wiley & Sons. Copyright © 2012 Wiley Periodicals, Inc.

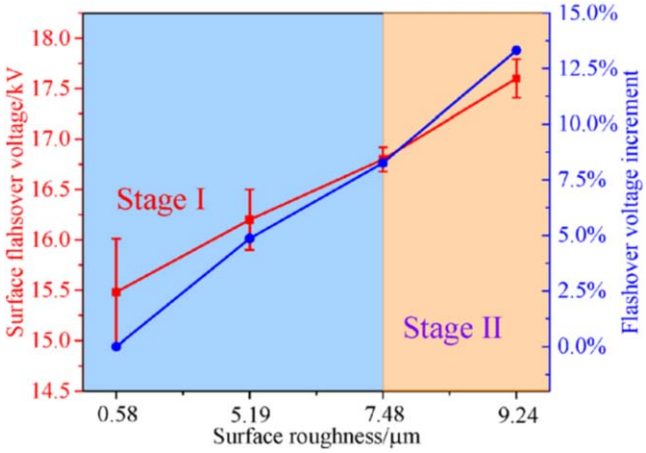

Figure 17. Surface flashover performance on spacer with different amount of surface roughness under positive DC voltage stress. Reprinted from [85], with the permission of AIP Publishing.

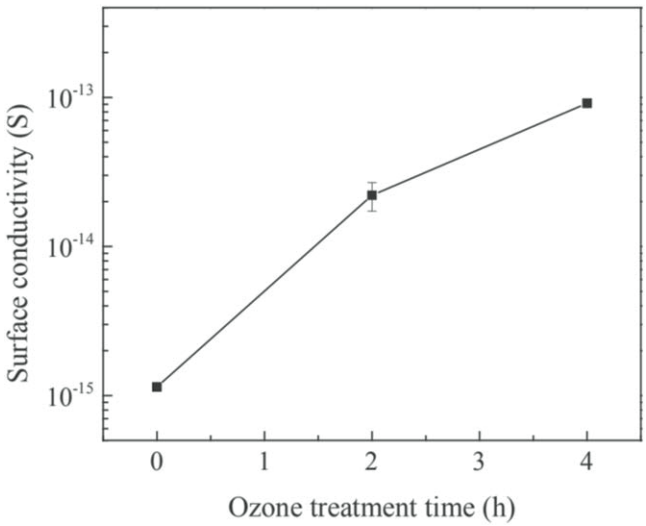

Figure 18. Surface conductivity of epoxy resin micro-composites before and after ozone surface treatment. © 2017 IEEE. Reprinted, with permission, from [50].

them on the surface. When they are cleared, the surface discharge occurs faster.

They performed a series of charging experiments with native polymers, as well as polymers doped with small amounts of chemical substances scavenging the radicals such as (as shown in figure 19(a)) (T)-a-tocopherol (vitamin E), bis(1-octyloxy-2,2,6,6-tetramethyl-4-piperidyl) sebacate (HALS), 2,2-diphenyl-1-picrylhydrazyl (DPPH) or 2,2-diphenyl-1-picryl hydrazine (DPPH-H), and the results showed that the presence of free radical scavengers reduced the tendency of the polymer to generate static electricity effectively during contact charging. Figures 19(b) and (c) show that under the corona discharge, the surface charge attenuation of the sample with added DPPH, is significantly higher than that of the original sample.

However, this radical scavenger approach may not work for thermosetting materials such as epoxy resins. We performed similar researches using astaxanthin, which serves as a strong oxidant, to treat epoxy based materials. The results showed that a good level of charge dissipation can only be found in samples just after treatment, and this charge dissipation ability gradually decreases with time. After storage for 24 h in air and in SF_6, we found that the surface potential decay rate becomes invalid with the same charge decay rate as that of the untreated samples (as shown in figure 20).

The charging mechanism of contact electrification-(triboelectrification) and electrification due to electric fields or corona are very different from each other. One involves material transfer, surface oxidation, reorientation of polar molecules; however the other involves mainly oxidation and may be reorientation. The impact of specific physical or chemical reaction processes on this event needs further research. In addition, in H. Tarik Baytekin 's study, they used PDMS, an elastomer with very low Tg, and molecules or chains were very active at the surface (and also in the volume) at the room temperature. For this reason, antioxidant molecules could find the active groups easily at the surface, and discharg occured rapidly. Epoxy may not have these characteristics.

3.4.5. Analysis and discussion. Table 5 shows the results obtained from different treatment methods in this section. It can be found from [50, 85] that compared with the roughness treatment that can increase surface conductivity by 1 order of magnitude, the ozone treatment effectively increases surface conductivity of nearly 2 orders of magnitude after treating the

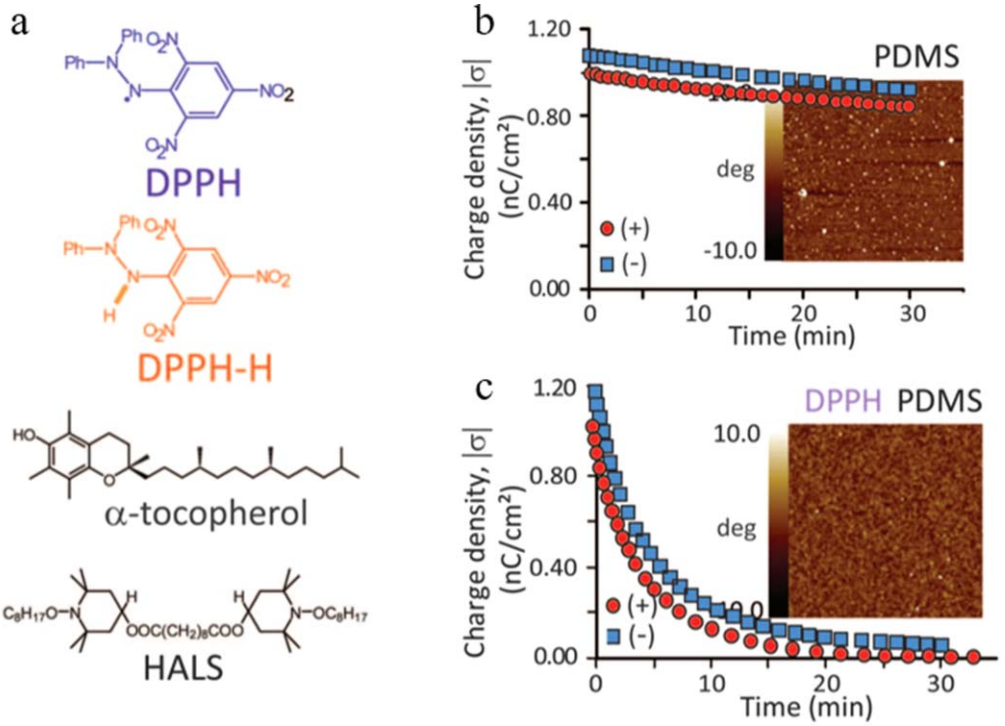

Figure 19. (a) Four kinds of radical scavengers; (b) charge decay of pure PDMS charged by corona discharge either (+) or (−), and free radicals(white spots) distribution of different samples in 30 min; (c) charge decay of PDMS/5 mM DPPH charged by corona discharge either (+) or (−), and free radicals(white spots) distribution of different samples in 30 min. From [51]. Reprinted with permission from AAAS.

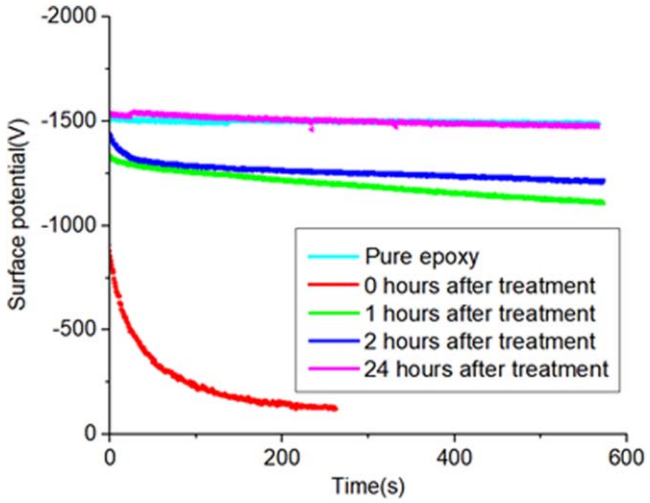

Figure 20. Epoxy surface potential decay curve of epoxy resin treated with astaxanthin and stored at 0.1 MPa SF_6 for different certain times (Soak for 10 min, test after drying).

sample for 2 h. Meanwhile, the increase ratio of the flashover voltage of samples by different treatments shows that the surface flashover voltage of the treated sample by roughness method was increased by 13.37%, while the surface flashover voltage of the ozone-treated samples is increased by 20.93%. It should be noted that due to the differences in samples and experimental setup, it would be difficult to make comparisons regarding surface flashover properties.

The radical scavenger treatment method uses the coexistence of these free radicals to achieve the purpose of eliminating charges indirectly by eliminating free radicals. However, for the radical elimination mechanism of epoxy based samples, more studies should be carried out. Meanwhile, the aging behavior and anti-aging property should be more important while dealing with products in industrial applications. Gamma ray shows very good property in surface charge decay rate. However, such methods are complicated and might threaten the human health if not been controlled properly. Besides, g-ray produces homogeneous modification of the material, meaning that both surface and volume leakage should be modified. The treatment may have detrimental effects to bulk insulation.

4. Dam reinforcement-suppressing charge from volume conduction and gas ionization

In order to decrease the conduction current from the volume, manners of coating or doping are usually used, while coating on the conductor surface and/or smoothing the conductor surface both can decrease micro discharge and thereby limit charges from gas ionization.

4.1. Suppressing charge from volume conduction current

In order to suppress charge from the volume, we focus on the metal/insulation interface as well as the bulk property.

4.1.1. Cr_2O_3 coating. A dense, ordered Cr_2O_3 nano-coating created by the magnetron sputtering method on the epoxy surface was verified as a good way to restrain charge injection from metal/insulation interface, which is due to deep traps introduced by the coating [34, 52]. The effect of fluorination,

Table 5. Modification methods and corresponding results of each research group.

Research group	No./ref	Treatment method	Parameter	Surface conductivity 10^{-18} S m^{-1}	Result	
					Surface potential decay ratio (at 1000s)	Flashover voltage kV (Increasing rate)
Gao	[48]	gamma-ray irradiation	Untreated		7%	
			100 kGy irradiation		10%	
			1000 kGy irradiation		15%	
Xue	[85]	Surface roughness treatment	Roughness:0.58 μm	5.8		15.5
			Roughness:5.19 μm	80.6		16.2 (+4.91%)
			Roughness:7.48 μm	99.0		16.8 (+8.27%)
			Roughness:9.24 μm	22.3		17.6 (+13.37%)
Min	[50]	Ozone treatment	Untreated	1100	20%	21.5
			Processing 2 h	25 000	100%	24.7 (+14.88%)
			Processing 4 h	90 000	100%	26.0 (+20.93%)

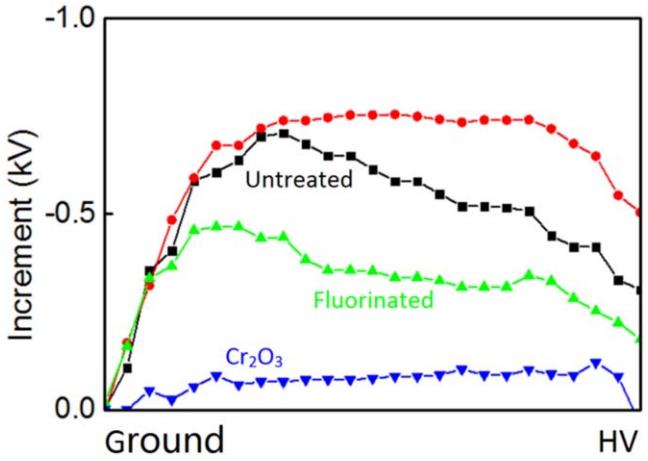

Figure 21. Surface potential increment from 0.5 to 2 min. Reproduced from [34]. © IOP Publishing Ltd. All rights reserved.

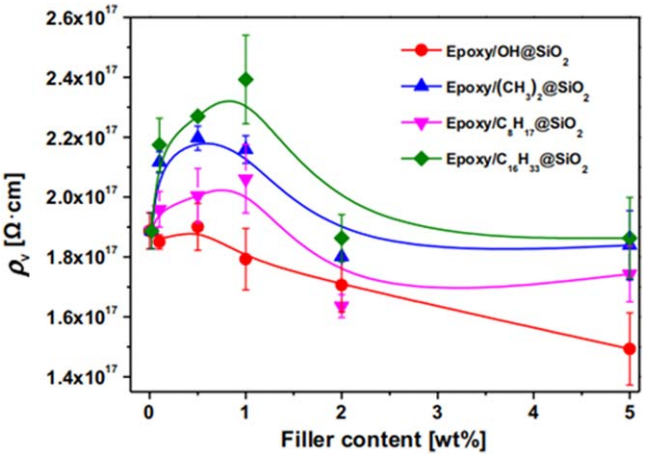

Figure 22. The volume resistivity (ρv) of epoxy and epoxy nanocomposites at room temperature ρv-filler fraction curves. Reprinted from [86], Copyright (2017), with permission from Elsevier.

plasma treatment, and Cr_2O_3 coating on charge suppression property using epoxy samples were compared and results showed that the Cr_2O_3 coating has the best charge injection suppression behavior, followed by surface fluorination as shown in figure 21 [34].

4.1.2. Nano-doping. Zhang *et al* verified that surface-modified silica nanoparticles can be used to suppress the leakage current of epoxy [86]. Figure 22 presents the variation of volume conductivity (ρv) of epoxy nanocomposites with different filler fraction and the results show that for the nonlinear change of the volume conductivity (ρv) of the alkyl-modified nanoparticles with the proportion of filler, the maximum ρv value is obtained at a low filling fraction (1 wt%). They believed that the effect of the volume resistivity on the surface modification of nanoparticles can be attributable to two possible reasons: (1) low-polarity nanoparticles have a large number of highly insulating alkyl groups and a small number of hydroxyl groups and/or absorbed water molecules (that is, charge carriers (ions) that increase conductivity under an electric field); (2) surface modification changes the Maxwell–Wagner–Sillars polarization behavior of the composite material, thereby affecting the electrical conductivity of the composite material.

Zhang *et al* introduced different contents of Buckminsterfullerene C_{60} into epoxy resin to limit the mobility of charge carriers in the material [53]. They found that the electrical conductivity of 100 ppm C_{60}/epoxy composite decreases dramatically with a value of 1.0×10^{-18} S cm^{-1}, which does not exceed 20% of the conductivity for pure epoxy resin. They believe that deep traps introduced are responsible for the inhibition of charge injection.

The above mentioned studies focused on methods to suppress charge injection. However, He *et al* focused on restraining the charge transport inside the bulk by doping $K_2Ti_6O_{13}$ whiskers into epoxy based material [54]. They took advantage of the thermal barrier effect of $K_2Ti_6O_{13}$ whiskers to suppress the transport of homo-polar charges in the bulk, and the result demonstrate that the introducing the $K_2Ti_6O_{13}$ whiskers can effectively restrain heat propagation due to its excellent thermal barrier property, which in turn limits charge transport effectively, especially at temperature gradient.

Table 6. Modification methods and corresponding volume conductivity of each research group.

Research group	References	Processing method	Sample composition	Ambient temperature °C	Doping amount	Volume conductivity 10^{-16} S m^{-1}
Zhang	[86]	Nano-doping	Epoxy/$C_{16}H_{33}$@SiO_2	20	0	5.26
					0.5	4.39
					1%	4.167
					2%	5.29
					5%	5.21
Zhang	[53]	Nano-doping	Epoxy/C_{60}	20–25	0	6.1
					1 ppm	4
					10 ppm	2.7
					24 ppm	2.2
					100 ppm	1.0
					200 ppm	1.2
					1000 ppm	6.9
He	[54]	Micron doping	Epoxy/Al_2O_3	12–14	0	58.48
			Epoxy/Al_2O_3/$K_2Ti_6O_{13}$		10%	96.15
			Epoxy/Al_2O_3/asbestos		10%	44 444.4

4.1.3. Analysis and discussion. It has been shown that C_{60} and SiO_2 nano-fillers can reduce the sample volume conductivity. As shown in the table 6, the best property of epoxy samples are obtained when the doping amounts of the C_{60} nano-filler and SiO_2 filler are 100 ppm and 1%, respectively. However, compared with doping of C_{60} and SiO_2, the doping with $K_2Ti_6O_{13}$ whisker takes advantage of its thermal barrier effect in effectively prevent the diffusion of heat under condition of temperature gradient.

4.2. Suppressing charge from gas phase

The electric field at the micro-protrusions on the rough electrode surface can be enhanced to a level under which micro-discharge will take place. Controlling the surface roughness of electrodes can effectively suppress the source of charge generated by the micro-discharge from the gas phase [87–89]. Figure 23 shows stabilized currents measured in both polarities with respect to electric field ranging from 2 to 30 kV · mm^{-1}, with electrodes A, B, and C, and fixed gas condition (0.6 MPa, 20 °C, RH ≈ 30%) [88]. In both polarities, currents are strongly influenced by the high voltage electrode roughness, with a two orders of magnitude difference between electrodes (A) and (C).

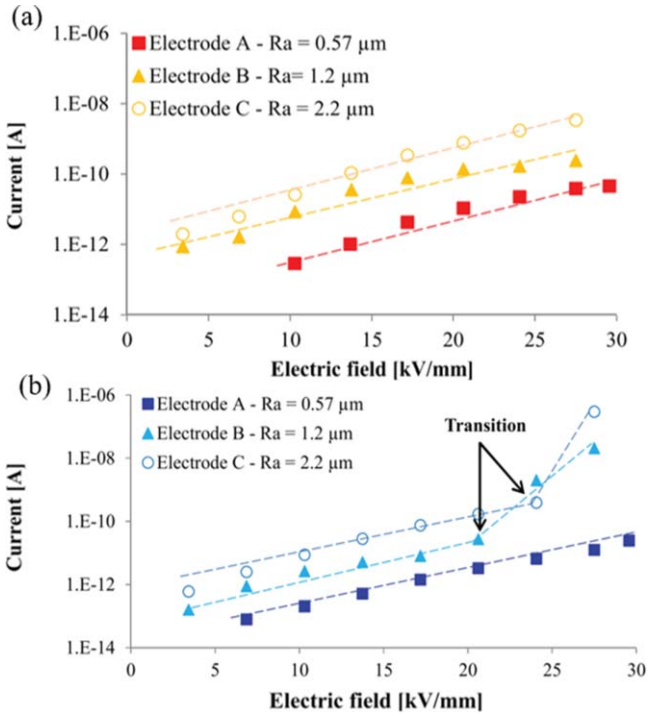

Figure 23. Current measured in SF_6, versus electric field for three different electrode roughnesses, (0.6 MPa, 20 °C, RH ≈ 30%) (a) in positive polarity; (b) in negative polarity. Reproduced from [88]. © IOP Publishing Ltd. All rights reserved.

5. Dredging-local electric field modification

Dredging is a commonly used approach to increase the canal depth and therefore increase the capacity of canals for carrying water. With respects to spacers, by means of material modification and shape controlling, local electric field can be optimized and the flashover withstand voltage of the spacer can thereby be increased. To achieve this goal, nonlinear materials are usually adopted to modify the local electric field, and shape modification of insulators can also be a good way to optimize local electric fields.

5.1. Nonlinear conductive composite

In 1999, Messerer *et al* coated dupont conductive powder which contains titanium oxide and tin oxide on the surface of epoxy resin. They found that the maximum value of the electric field on the surface of the insulator is reduced from 36.7 to 29.6 kV cm^{-1} under the DC voltage of 100 kV after coating on a cylindrical sample of polyethylen with a diameter of 2 cm [90]. When the surface conductivity of the insulator is increased to 10^{-11}–10^{-12} S, the electric field

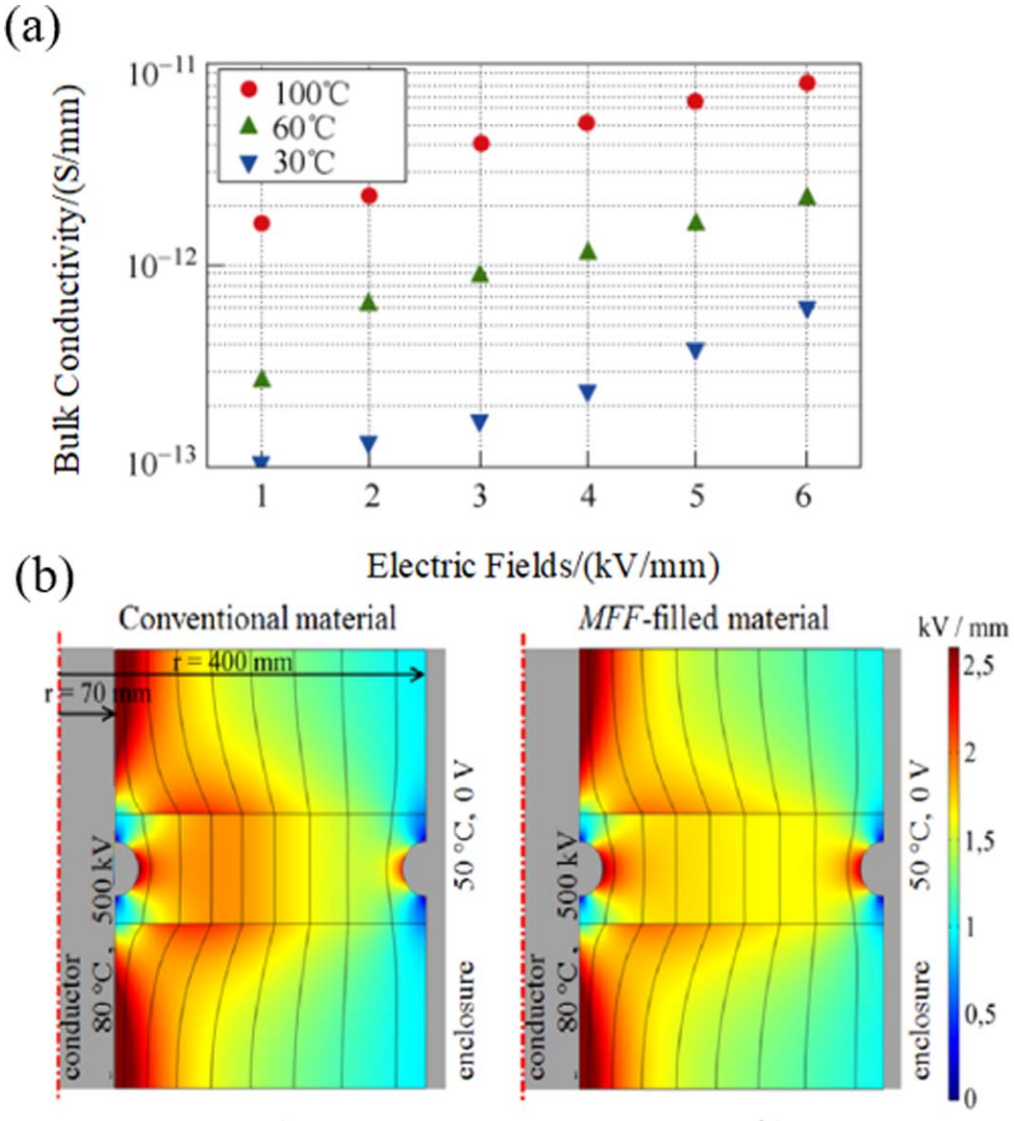

Figure 24. (a) Bulk conductivity of MFF-doped epoxy under different electric fields and temperatures. Reproduced with permission from [94]; (b) electric field distribution of conventional insulator and MFF-filled insulator. Figure reprinted with permission from CIGRE, [92], © 2015.

distribution on the surface of the insulator can be effectively improved [91]. Based on the preliminary conclusion on electric field optimization taking advantage of distributed conductivities, nonlinear conductivity composites, which have nonlinear behavior with respect to the electric field, are considered by researchers worldwide. This chapter mainly reviews the application of nonlinear materials in the modification of local electric fields.

5.1.1. Bulk doping. In 2013, Tenzer *et al* proposed an insulator using oriented 'MFF (Minatec® functional filler)' filler [92, 93]. These commercially available particles are flake-shaped mica pigments, covered by a thin tin oxide layer doped with antimony and titanium dioxide. Figure 24(a) shows that such MFF-doped epoxy composites have good nonlinear conductivity properties related to electric field strength [94]. Meanwhile, the electric field distribution of MFF-doped insulators presented in figure 24(b) shows a more uniform electric field distribution on the surface under the effect of room temperature and temperature gradient than the traditional spacer.

Du *et al* studied effect of SiC particles on electrical characteristics [64, 66] and the results showed that with the increase of the filler content, the threshold value of nonlinear conductivity has a downward trend, with their values of 8, 2.8 and 2 kV mm^{-1} for samples with doping ratios of 3, 10 and 14 vol% as shown in figure 25(a) [64]. They further found that with the increase of temperature, the flashover voltage of untreated samples becomes higher than SiC-doped samples, as shown in figures 25(b)–(d) [66].

Surprisingly, an opposite trend was reported regarding insulators doped with SiC [67]. As shown in figure 26, the DC flashover voltage at 0.4 MPa SF_6 gas of cone type insulators and post type insulators with different SiC contents has descending trend, except for cone type insulator with doping ratios of 20% and 25%.

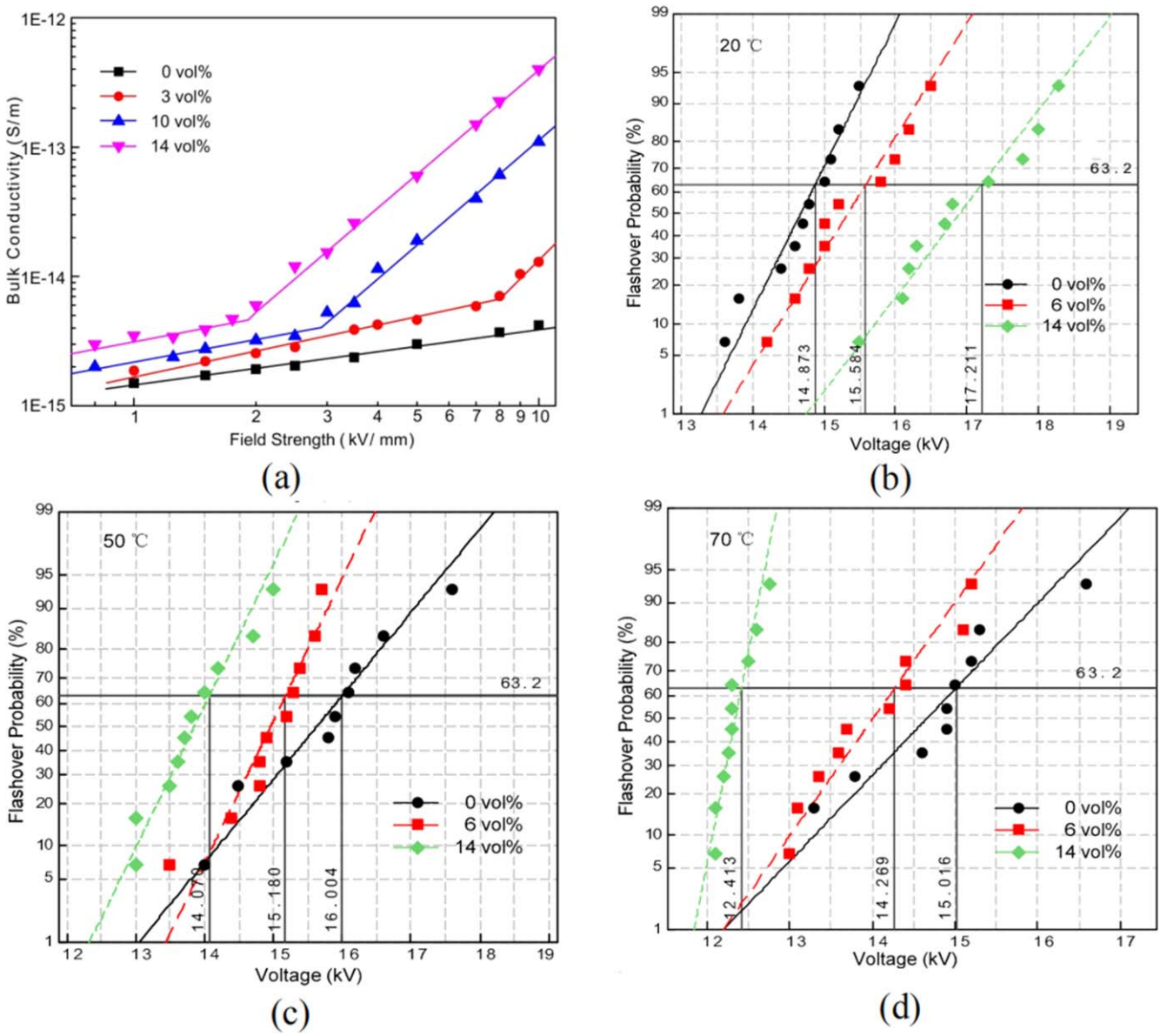

Figure 25. (a) Relation between the bulk conductivity and the electric field strength. © 2018 IEEE. Reprinted, with permission, from [64], (b) the flashover voltages of samples with different filler contents at 20 °C, (c) the flashover voltages of samples with different filler contents at 50 °C, and (d) the flashover voltages of samples with different filler contents at 70 °C. © 2018 IEEE. Reprinted, with permission, from [66].

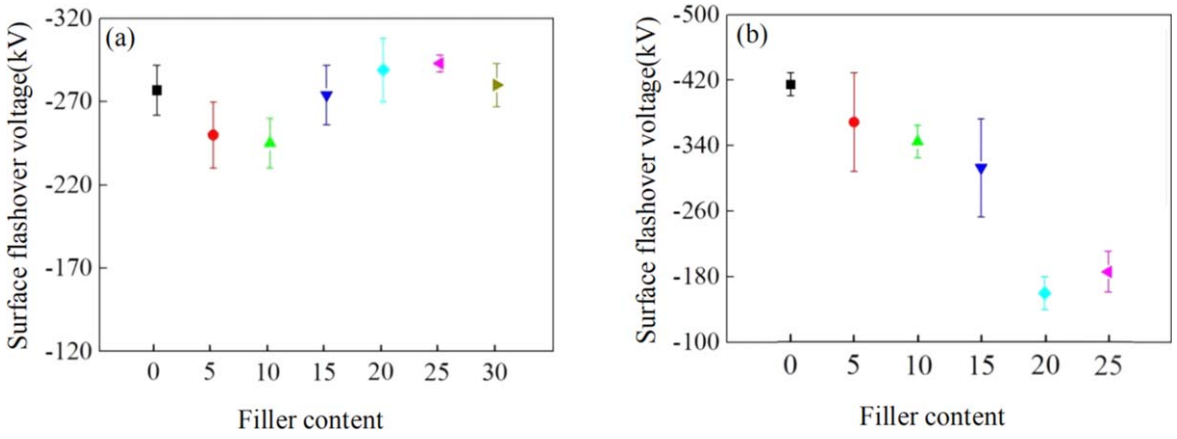

Figure 26. DC surface flashover voltage values of insulators with different mass fraction of SiC particles. (a) cone type insulator model and (b) post type insulator model [67].

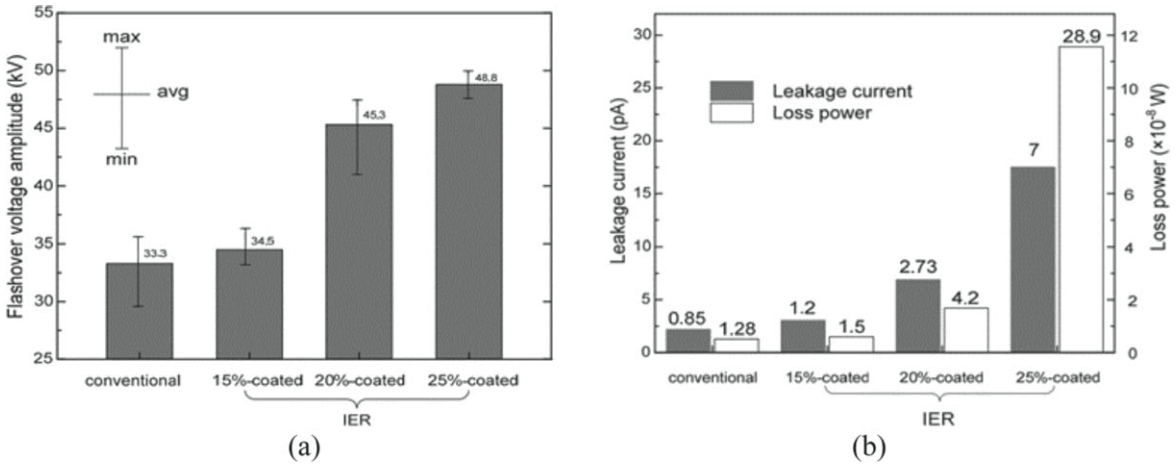

Figure 27. (a) Measured flashover voltages of the conventional insulator and IER insulators with different SiC contents and (b) leakage current and loss power of the IER insulators with different filler contents. © 2019 IEEE. Reprinted, with permission, from [68].

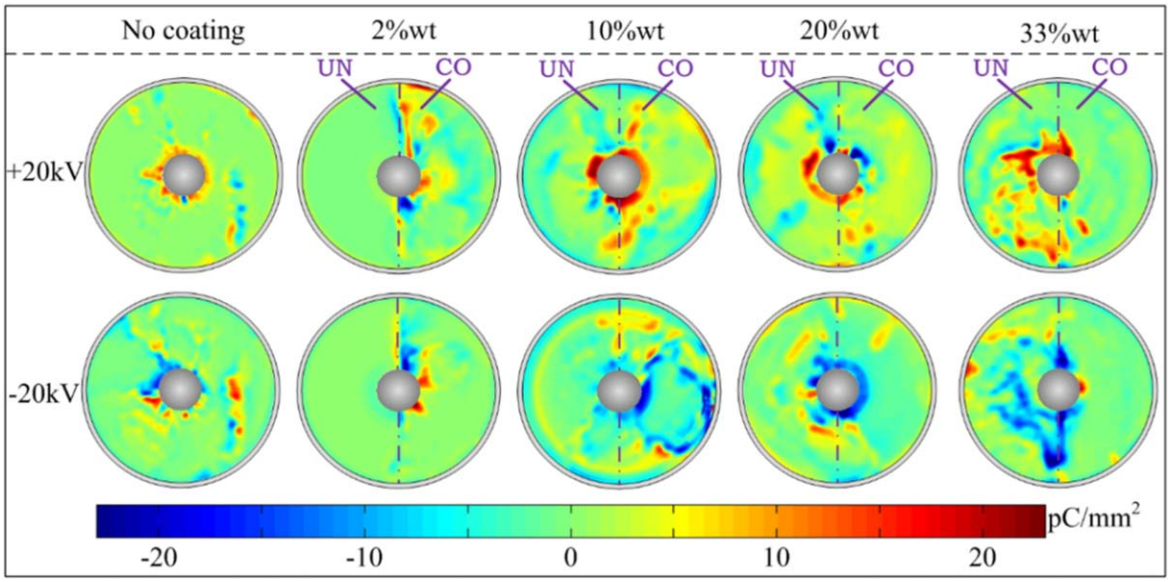

Figure 28. Surface charge distribution patterns with different SiC contents. Reprinted from [69], Copyright (2020), with permission from Elsevier.

5.1.2. Surface coating. ZnO is deposited on epoxy surface by a magnetron sputtering to prepare functional gradient surface layer [65] and the surface flashover voltage was improved significantly. Subsequently, the concept of the interfacial electric field self-regulating (IER) insulator was put forward and the tapered insulator with EP/SiC composite material was prepared as the IER insulator [68]. β-SiC ring-clad insulators with different doping contents (15%, 20%, and 25%) were prepared and DC surface flashover voltage in the medium of 10%–90% SF_6/N_2 mixed gas at 0.1 MPa was tested. Figure 27(a) shows the DC flashover voltage results. The flashover voltage of EP/SiC coated insulator is higher than conventional insulators, and the surface flashover voltage increases with the increase of SiC content. However, for EP/SiC-coated insulators with higher SiC content, the reduced volume resistivity of the EP/SiC coating results in higher leakage current and power loss (as shown in figure 27(b)).

Apart from that, Xue *et al* sprayed a non-linear conductive coating composed of SiC filler and epoxy on the insulator surface [69, 70]. The surface charge distribution patterns under DC voltages with different SiC contents are displayed in figure 28 [69]. With the increase of SiC content, surface charges show firstly an increasing and then a decreasing trend.

As an example for the positive flashover test in air at 0.1 MPa, the positive flashover voltage is non-linearly distributed by increasing the SiC content. They divided this phenomenon into three stages: the decline stage (0%–10% wt), the improvement stage (10%wt–33%wt), and the degradation stage (33%wt–50%wt), as shown in figure 29. When the content is 33%wt, the flashover voltage shows the highest value.

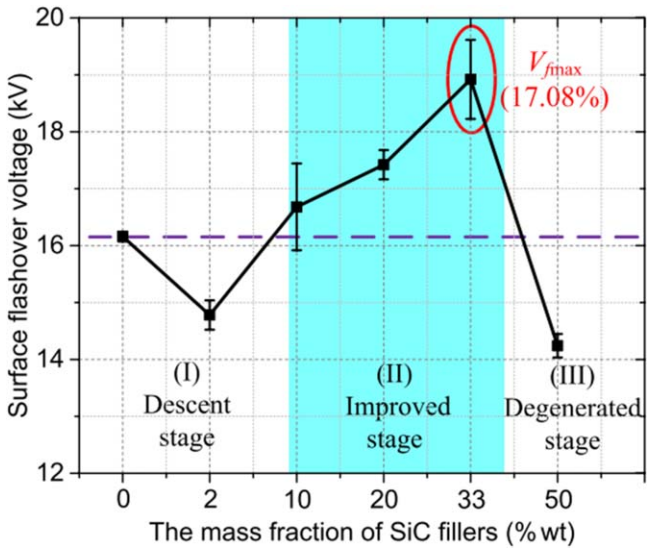

Figure 29. Surface flashover in 0.1 MPa air on SiC/epoxy coated spacers with different SiC mass fractions. Reproduced from [70].

Then Xue *et al* turned their attention to the influence of SiC particle size in SiC/epoxy coating [71]. As shown in figure 30, the results showed that surface charges are significantly suppressed by SiC/epoxy coatings, especially using smaller SiC particle size. Flashover voltage in 0.1 MPa 20% SF_6/N_2 mixtures increases gradually with decrease of SiC particle size.

Then they proposed surface conductivity graded coating (SCGC) scheme to overcome the drawbacks of entire coating manner [9]. Four kinds of surface graded coating schemes are considered, as shown in figure 31.

The surface flashover tests are conducted on raw alumina/spacers and with different SCGC schemes when SiC content is 10%wt. The results are shown in figure 32. The result shows that HV-coating has the best effect in increasing of surface flashover voltage.

Tang *et al* prepared epoxy matrix composites with different contents of nano-SiC particles to coat on epoxy resin [72]. Figure 33 shows the surface trap distribution of samples with and without additive of nano-particles. With the SiC particles doping, shallow traps were introduced, leading to an evidently decline of trap energy level, which would be beneficial to the process of charge de-trapping and extraction.

5.1.3. Analysis and discussion. In this section we chose representative results from the above mentioned research groups for comparison and discussion. Table 7 summarizes the effect of nonlinear conductive composite modifications on the surface potential decay rate and flashover voltage based on the available literature. As it can be seen, a wide range of parameters including shape of sample, processing method, test environment, doping amount and applied voltage could directly influence on the results. In literature [64], a direct relationship between doping amount and surface potential decay rate which shows increase of the doping rate for square sheet sample and under positive applied voltage leads to surface potential decay rate enhancement was presented, however, this relation for disc sheet samples and under negative voltage can not be seen. Literature [66] shows that temperature rise increases the rate of surface potential decay for the same doping amount except for 14% doping at 70 °C. Moreover, the presented results in [68] describes the flashover voltage enhancement with the growth of doping amount for conventional insulator. Zhang *et al* investigated the doping amount from 0% to 50% for cone type spacer and coating processing and the results show the maximum flashover voltage happens at 10% doping. Literature [67] studied the flashover voltage for different doping amount from 0% to 30% for two types of samples including post type and cone type insulator; for post type insulators, doping decreases the flashover voltage, yet 25% doping causes 4.6% growth of the flashover voltage for cone type insulator.

Meanwhile, regarding the surface flashover voltage at different temperatures, the temperature dependent conductivity should be very important since it affects the charge decay rate significantly, resulting in a changing the surface flashover dispersion. However, problems lie in the difficulty of measuring the surface conductivity at high field and high temperatures since surface flashover would be triggered even at very low field (i.e. 30 kV mm^{-1}), during surface conductivity measurement, even for well protected and polished electrodes. Meanwhile, in consideration of practical applications, most studies conducted tests at low pressure, which the electric field cannot reach that high compared with the real cases where the gas pressure reaches 0.4 MPa or more. For non-linear materials, due to its property sensitivity with respects to electric field variations, testing under operating conditions must be considered. In addition, the long term aging test and material property variation under transient pulses should further be performed.

5.2. Shape improvement

Apart from introducing nonlinear materials which modifies local electric field decently, modifying the profile of insulator to adjust the electric field line distributions can also be a useful approach to suppress charge accumulation and realize local field improvement. In 1982, Cooke found that the charging of the insulator would be associated with a particular nearby source [2], and he believed that the overall geometry of insulators plays an important role in surface charging. Similar conclusions were also presented in his early papers [58, 95]. Since Cooke's 1982 paper, the surface charge accumulation phenomenon has been highlighted by researchers using different model spacers.

5.2.1. Literature review. In 1983, a very detailed study on surface charging phenomenon and mechanism was conducted by Nakanishi *et al* [59]. Based on their experimental results [2, 59], Fujinami put forward an anti-charging spacer model that has no normal field component over the surface, as shown in figure 34 [57].

After 1988, the investigation of surface charge transport in real-sized spacers accelerates the research progress in exploring the surface charge transport mechanism [55, 56].

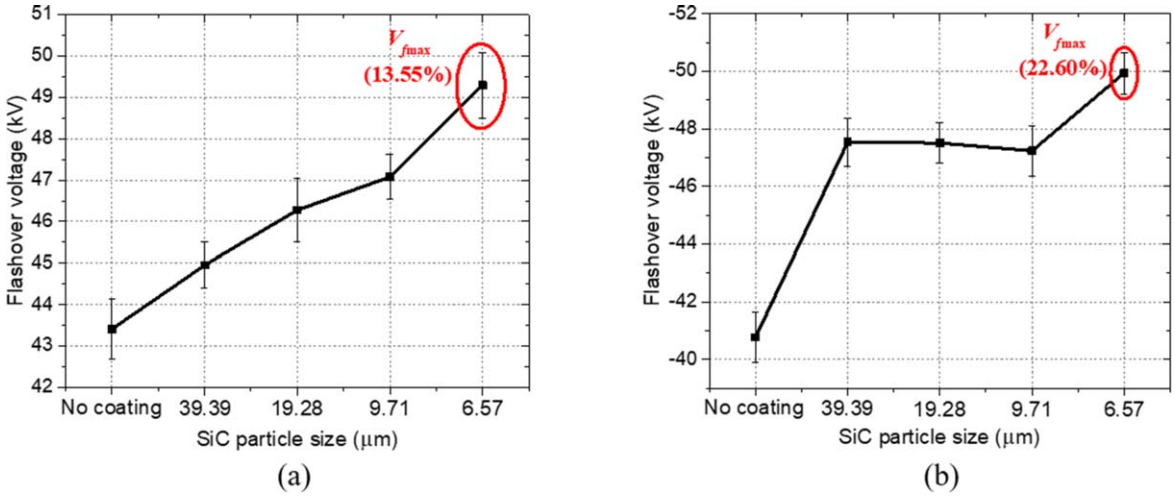

Figure 30. Flashover voltage of SiC/epoxy coated alumina/epoxy spacers with different SiC particle size in 0.1 MPa 20% SF_6/N_2 mixtures. (a) Positive DC. (b) Negative DC. Reproduced from [71]. © IOP Publishing Ltd. All rights reserved.

However, the implementation of industrial application of HVDC spacers has still been hampered by the non-reproducibility of some experimental results and difficulties in interpreting the surface charge distribution of field measurements. In 1991, Nitta and Nakanishi introduced a design principle that states that the surface of the spacer should intersect the electric field lines at an angle as acute as possible so as to reduce the normal electric field component as much as possible [56]. Based on their design idea, cone type spacer and post type spacer for ±500 kV GIS were manufactured, as shown in figure 35.

Figure 36 shows the combined field strength *E*, field strength tangential component *Et* and field strength normal component *En* calculated by Hasegawa *et al* for the design of a 500 kV DC GIS bus in 1997 [60]. It can be found that the *En* of the semi-conical basin insulator is lower than that of the conical insulator, which can effectively suppress the accumulation of surface charges.

In 2004, Volpov summarized the general criteria for reliable insulator performance in high-voltage DC gas insulation systems [61], and proposed generalized design criteria for HVDC insulators. He believed that the first principle for the optimal design of columnar insulation structures is that the maximum value of the electric field strength along the insulator is smaller than the insulation margin. In this basic principle, the initial normal electric field strength on the gas side of the solid–gas surface should be as small as possible. Meanwhile, for the cone type insulator, the maximum value of the initial normal electric field strength and the initial tangential electric field strength distinctively should be less than the threshold. His research results provide quantifiable design criteria for insulator design applied in HVDC GIS.

Jia *et al* focused on the comprehensive influence of the material and shape of the insulator on its flashover characteristics under DC voltage. Figure 37 shows insulators with different shapes used for experimental comparison [63]. The result showed that the flashover voltage of the umbrella skirt insulator was the highest at each pressure.

In our recent research [62], a criterion was put forwordwhich focused on the balance of tangential and normal electric field compments along the surface of insulators. And a novel HVDC cone-type insulator was developed, as shown in figure 38.

The novel DC cone-type insulator passed a series of tests according to standards in gas-insulated equipment [62], which provided a better performance than the traditional AC insulators in the same voltage level. It is noted the flashover voltage of the novel insulator under DC superimposedlightning inpluse voltage, exceeded the evaluation standard. in the 1:4 SF_6/N_2 gas mixture at 0.7 Mpa.

Meanwhile, a ±200 kV spacer as shown in figure 39, was further developed. Comparison between the 200 kV dc spacer and a 220 kV AC spacer was performed by DC surface flashover and polarity reversal tests at 0.3 MPa SF_6 (as shown in figure 40). For DC spacer, the surface charge density of convex surface is lower than 10 $\mu C\,m^{-2}$, and that of concave surface is lower than 5 $\mu C\,m^{-2}$. For AC spacer, the surface charge density of concave surface is higher than 10 $\mu C\,m^{-2}$, and it even reaches to 18 $\mu C\,m^{-2}$ on the convex surface. The flashover voltage of AC and DC spacers are both lower than that in the DC linear-boost test. The flashover voltage of AC spacer after polarity reversal decreases more than that of DC spacer, from 420 to 440 kV to less than 360 kV. In addition, the linear-boost flashover voltage of DC spacer is slightly higher and more stable than the AC spacer. The polarity reversal flashover voltage of DC spacer is slightly lower than the linear-boost flashover voltage.

One difficulty with gas-insulated components under DC stress is to predict the field distribution in the solid spacers and in the gas in the vicinity of the spacers. DC spacers must be able to withstand not only long time DC stress but also switching and lightning overvoltages and DC polarity reversal. All these factors have to be considered when DC spacers are designed. There is therefore a need to develop methods to investigate charge accumulation and field distributions on spacer surfaces. As a charging counter measure surface coating of insulators was introduced for the first time. The spacers used were made of a standard epoxy

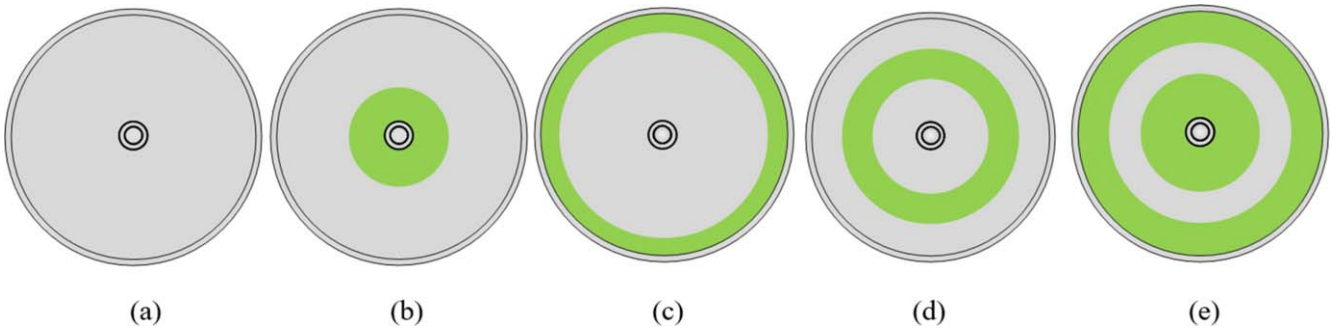

Figure 31. Different surface graded coating schemes. (a) Raw spacer. (b) High conductive coating locates close to HV electrode (HV-coating). (c) High conductive coating locates close to GND electrode (GND-coating). (d) High conductive coating locates at the middle of spacer surface (SPM-coating). (e) High conductive coating locates close to both HV and GND electrode (HV-GND-coating). Reproduced from [9].

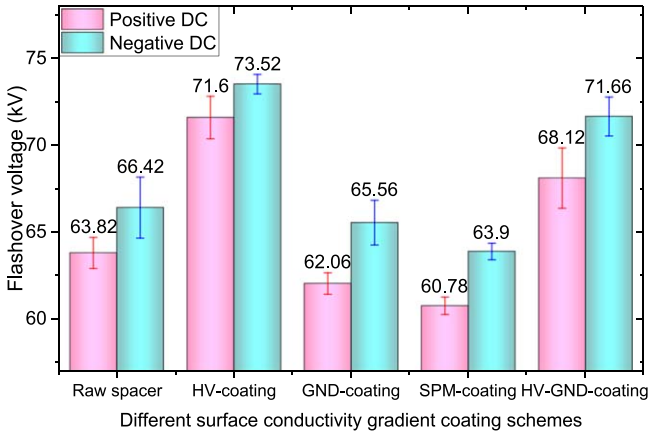

Figure 32. Surface flashover voltage with different SCGC schemes. Reproduced from [9].

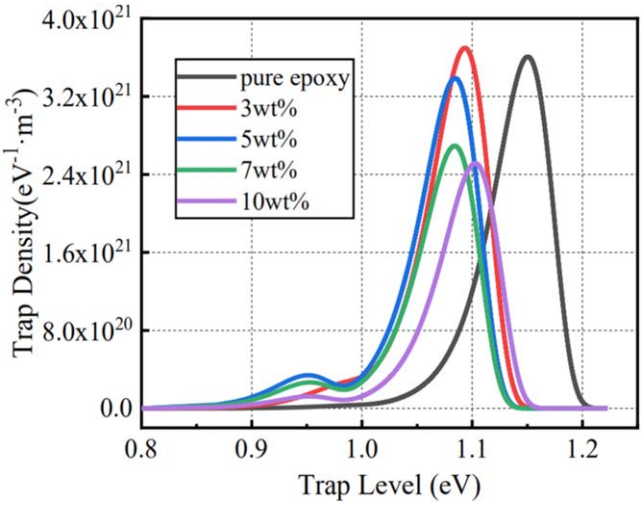

Figure 33. Surface trap distribution of nano-SiC/Epoxy composites. Reproduced from [72].

with alumina filler. Some of the spacers have been covered with a slightly conducting film. The spacer surfaces were cleaned with alcohol before mounting. This treatment gave charge-free surfaces. The potential shift for the covered spacers reached its equilibrium faster in a few days. After polarity reversal, the potential shift reversed and reached steady state with the same time constant as before. In figure 41 a summary of obtained results for both coated and uncoated spacers is shown. The faster re-distribution on the coated spacers documents that in this case surface conduction is the dominant process. As a summary the results from the 1980s obtained for uncoated and coated surfaces indicate that suitably chosen surface coatings can be used to control the field distribution at the surface of solid spacers under HVDC stress, making SF_6 insulated components feasible in HVDC applications as well as in HVAC.

Another approach to avoid charge accumulation is to make the resistive field distribution equal or similar to the capactive field distribution by design and proper choice of material properties [57, 96–98]. The influence of temperature and temperature distribution must be considered.

The magnitude of the electric field at the solid–gas insulation interface (gas side) for various ion densities is shown in figure 42. For short times, the capacitive field (denoted AC) is tangential to the surface, resulting in a negligible ion capture volume and a maximum field located near the HV conductor. In contrast, for the DC steady state (no ion case), the presence of a temperature gradient across the insulation enhances the field in the less conductive region, i.e. near the grounded tank. For the same reason, DC field lines in the gas toward the solid have now a normal component and build up a capture volume for ions [99].

Based on the research for material characterization and the usage of multi-physics simulation tools the analysis of electrical field distribution is now possible with high precision, taking the following parameters into consideration: temperature and electrical field dependent characteristics of the used insulating materials, accumulation of space- and surface charges and the superposition of DC and impulse voltages [100]. Hence, the comparison between capacitive and steady-state resistive electric field strength distribution (gas side) for the HVAC partition insulator (figure 43) and the new developed HVDC partition insulator (figure 43), shows lower dielectric stress on the DC-design and under DC with some minor drawback in the case of AC [11].

For the optimized HVDC design, the improvement shown with a significant reduction of the dielectric stress was obtained by geometrical optimization and insertion of a

Table 7. Nonlinear conductive composite modification methods and corresponding results of each research group.

Research group	References	Sample shape	Treatment method	Test environment		Doping mass ratio	Results			
							Surface potential measurement		Flashover voltage test	
				Temperature °C	Relative humidity		Applied voltage kV	Surface potential decay ratio at 1200 s	Environment	Flashover voltage kV (Increasing rate)
Du	[64]	Square sheet	Doping	20	30%	0	+8	5%	Air 0.1 MPa	—
						3%		7.5%		
						10%		31.5%		
						14%		38.1%		
	[66]	Disc sheet		20		0	−7	19.51%		14.9(0)
						6%		15.8%		15.6 (+4.8%)
						14%		51.9%		17.2 (+15.7%)
				50		0		84.37%		16.0(0)
						6%		29.73%		15.2(−5.1%)
						14%		91.3%		14.1 (−12.0%)
				70		0		100%		15.0(0)
						6%		81.48%		14.3(−5.0%)
						14%		60.78%		12.4 (−17.3%)
	[68]	Conventional insulator	Coating	25	—	0	—	10%SF_6/N_2 0.1 MPa	33.3(0)	
						15%			34.5 (+3.6%)	
						20%			45.3(+36%)	
						25%			48.8 (+46.5%)	
Zhang	[70]	Cone type spacer	Coating	10–15	<10%	0		20%SF_6/N_2 0.1 MPa	−45.0(0)	
						2%			−40.0 (−11.1%)	
						10%			−54.0 (+20%)	
						20%			−53.0 (+17.8%)	
						33%			−34.0 (−24.4%)	
						50%			−30.0 (−33.3%)	
He	[67]	Post type insulator	Doping	—		0		SF_6 0.4 MPa	−420(0)	
						5%			−360 (−14.3%)	

Table 7. (Continued.)

Research group	References	Sample shape	Treatment method	Test environment		Doping mass ratio	Results			
							Surface potential measurement		Flashover voltage test	
				Temperature °C	Relative humidity		Applied voltage kV	Surface potential decay ratio at 1200 s	Environment	Flashover voltage kV (Increasing rate)
						10%			−340 (−19.0%)	
						15%			−320 (−23.8%)	
						20%			−160 (−62.0%)	
						25%			−180 (−57.1%)	
	[67]	Cone type insulator				0		SF_6 0.4 MPa	−280(0)	
						5%			−245 (−12.5%)	
						10%			−243 (−13.2%)	
						15%			−270 (−3.6%)	
						20%			−290 (+3.6%)	
						25%			−293 (+4.6%)	
						30%			−280(+0%)	

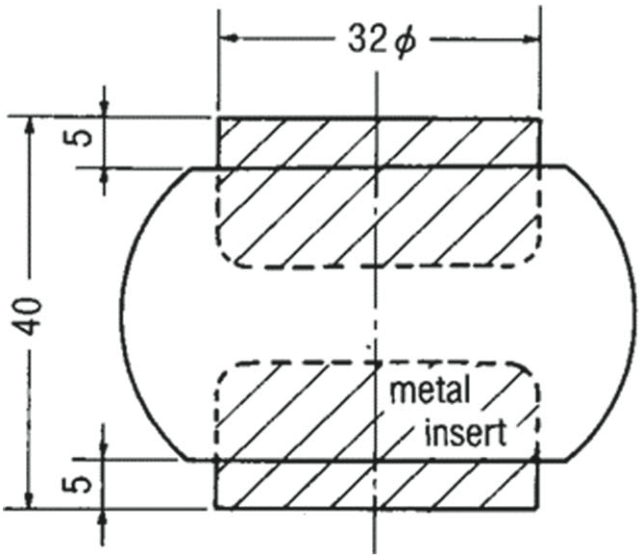

Figure 34. Spacer model designed by Fujinami. © 1989 IEEE. Reprinted, with permission, from [57].

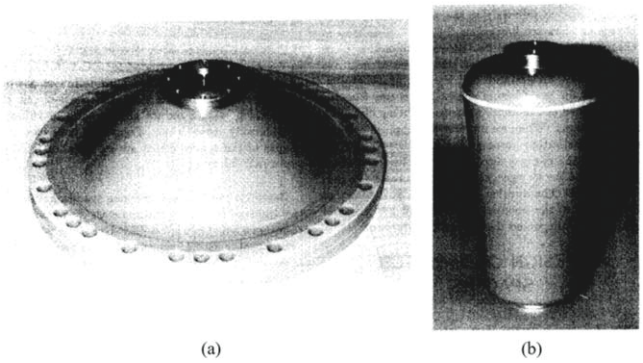

Figure 35. Spacer for ±500 kV HVDC GIS. (a) Cone type spacer and (b) post type spacer. © 1991 IEEE. Reprinted, with permission, from [56].

current collector, compared to the AC design. © 2016 IEEE. Reprinted, with permission, from [101]. The temperature gradient across the insulation considered for the simulation is equal to the worst case under service conditions and maximum continuous current.

5.2.2. Analysis and discussion. Shape modification as an approach to suppress surface charge accumulation of the insulator has advantages such as simple operation process and high reliability, which is preferred by manufactures. The temperature dependent conductivity may influence electric field distributions at DC, which results in irregular charge behaviors. This issue should be considered carefully. Currently, we see some favorable evidences regarding manufacturing of HVDC spacers, as is discussed in [11, 62, 101], however, it is still a pity that no design margin used for qualifying a charge density as well as a electric field stress/normal component value that is acceptable for the stable operation of HVDC spacers. This unfavorable situation is mainly due to the lack of knowledge regarding mechanism of charge triggered surface flashover at DC

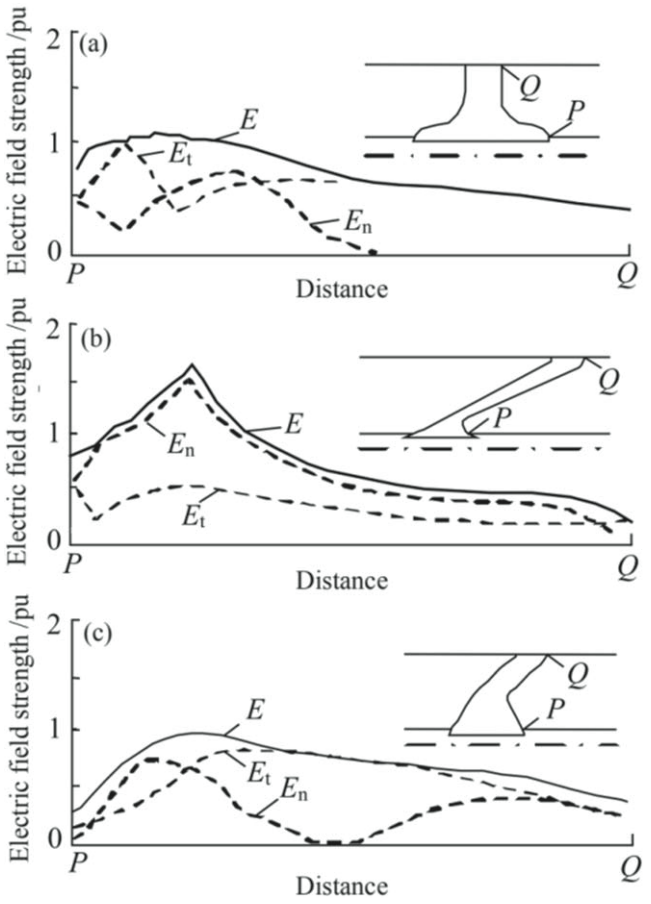

Figure 36. Distributions of electric field and its components on spacer surface concave side. (a) Disc-basin spacer, (b) cone -basin spacer, and (c) half conical-basin spacer. © 1997 IEEE. Reprinted, with permission, from [60].

voltage. Some footprints explaining charge-induced flashover are discussed in [14, 17]. However, there is a long road ahead for us before filling this research gap.

6. Comprehensive management-initiatively charge decay method

A novel design of HVDC spacer (shown in figure 44) was introduced based on the concept of adaptively controlling surface charges using nonlinear materials. This method, unlike commonly used traditional approaches, proposed a novel idea of controlling the location of accumulated charges and then properly decaying of these charges, which fundamentally solves the problem of surface charge accumulation. The electrical and mechanical test results show that the charge adaptively controlled spacer has high operating capability under DC voltage and has great industrial application potential [73–76].

The charge adaptively controlled spacer with a mass ratio of 20% SiC in the insulation region and 30% SiC in the charge adaptively controlled region shows the best results as indicated in figure 45 [76].

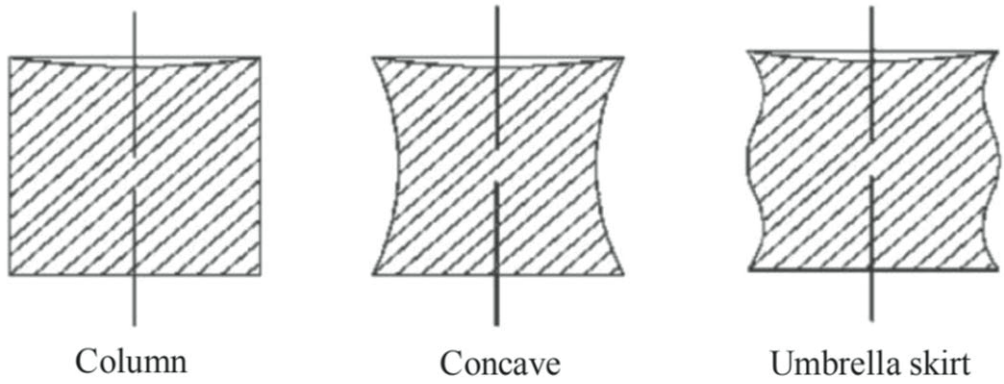

Figure 37. Three different shapes of insulators. Reproduced with permission from [63].

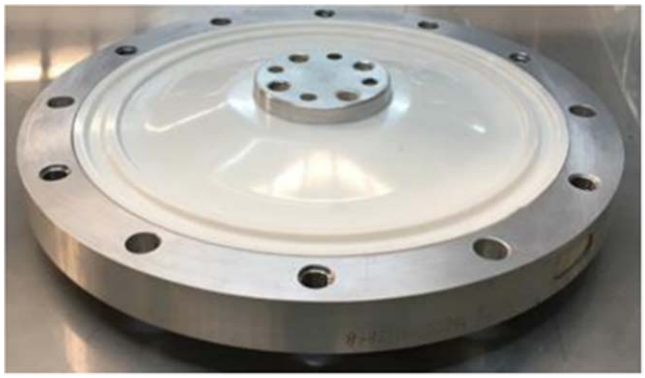

Figure 38. ±100 kV novel DC cone-type insulator. © 2019 IEEE. Reprinted, with permission, from [62].

7. Challenges and suggestions for future work

7.1. Surface charge origin and models

Before choosing the charge tailoring methods, we should firstly clarify the charge type we were to deal with, i.e. the homo-polarity charge due to conduction current and/or the hetero-polarity charge from the gas. Under this premise, we can regulate the charge in a targeted manner. Recently published research proposes a fairly convincing field-dependent charging theory, as has already discussed in the introduction, which can serve as a reference for ways determining charge origins [16].

Based on the charge origins, this paper introduces a Dam-flood model and classifies the surface charge tailoring methods proposed by different researchers. However, during chemically changing the surface conductivity, which has been verified to be an important way changing surface flashover voltage, the surface morphology is usually changed. This makes it difficult for us to discern what parameter plays a decisive role in surface flashover voltage improvement. For example, in the fluorination process, is it the morphology optimization or the increase of conductivity that really contributes to the surface flashover improvement? Further, surface conductivity determines surface charge dissipation performance, which is an important parameter that has been evaluated in the scheme by researchers. However, results obtained by previous researchers showed different conductivity values that make it impossible to compare and find the optimal margin to determine a suitable surface conductivity suitable for industry application.

Figure 46 presents the surface conductivity of epoxy based samples before and after surface modification [25, 32, 33, 42, 43, 45, 50, 85, 90]. It is worth noting that the surface conductivity of the base material without modification defers significantly, which ranges from 9.7×10^{-22} to 3.4×10^{-14} S. Surface modification increases surface conductivity and better surface property can be obtained. Further, we can see that fluorination results in a surface conductivity ranging from 8.6×10^{-19} to 9×10^{-14} S, which is relative lower compared with plasma treatment. However, coatings introduce a surface conductivity up to 1.11×10^{-9} S which is much higher compared with other surface modification methods. Surface roughness and ozone treatment increase surface flashover voltage while the trivial surface conductivity change is shown.

Such large difference over results in surface conductivity, to our knowledge, can be partially due to differences in test setup and environment condition (i.e. air pressures, ambient gases), electrode arrangement, electric fields, etc. Meanwhile, as a variable material which shows different properties produced by different companies, epoxy resin may probably be another factor responsible for such variations in measurement results. We would suggest that all tests and measurements to be based on practical industrial applications, and the test environmental condition should strictly follow the industrial application environment. In addition, there are various methods for characterizing material properties, and there is still a lack of unified measurement standards. Even if the same epoxy resin and the same processing technology are used, the conductivity measured by each research group is different, and some are several orders of magnitude different. (For example, the untreated epoxy conductivity measurement An and Chen's group are different [20–22, 28, 29], and after the same treatment method, the surface conductivity of fluorinated samples such as He and Du have a greater difference [31–33]). Such dispersion makes it difficult to compare and evaluate the effectiveness of a certain treatment method, which hinders the selection of surface conductivity during the preparation of insulators operating under DC voltage. It is necessary that the same measurement methods

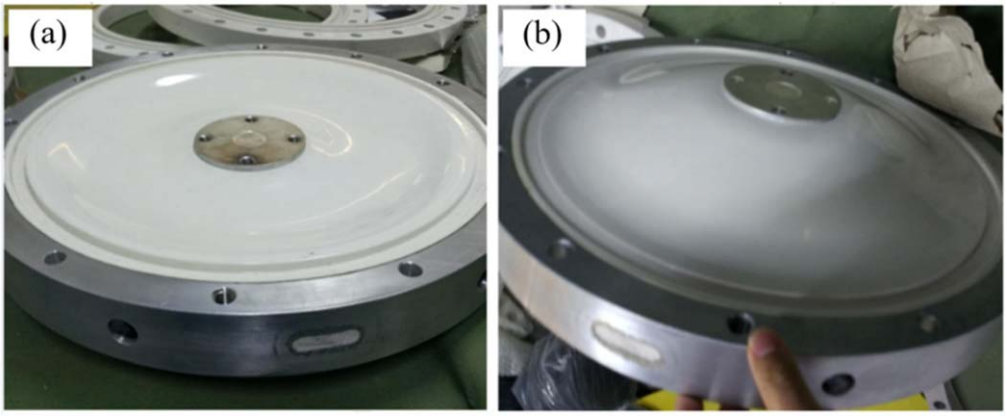

Figure 39. Physical pictures of the DC spacer. (a) Concave surface side and (b) convex surface side.

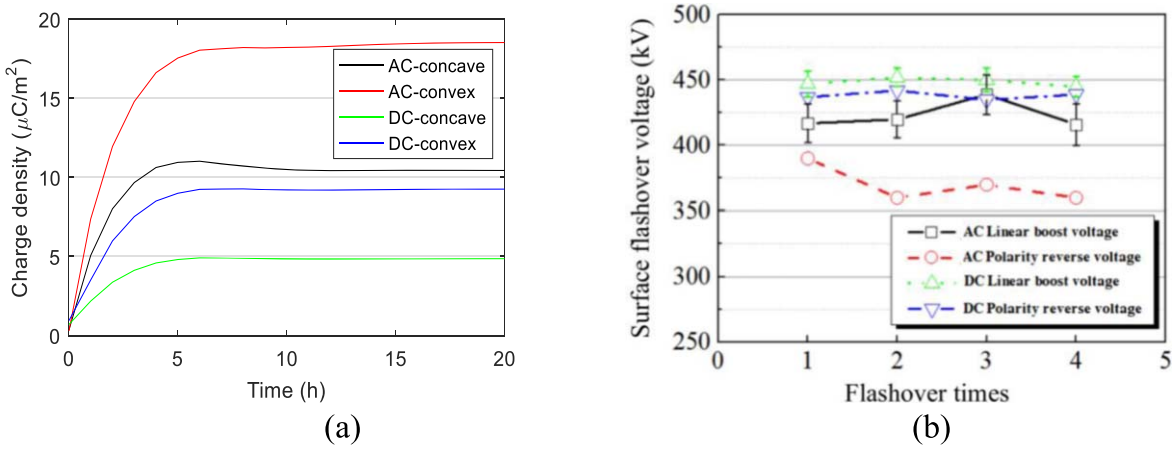

Figure 40. (a) Time varying curves of surface charge density along the surface of AC and DC spacers after applying 240 kV voltage, and (b) surface flashover voltage test results at 0.3 MPa SF_6.

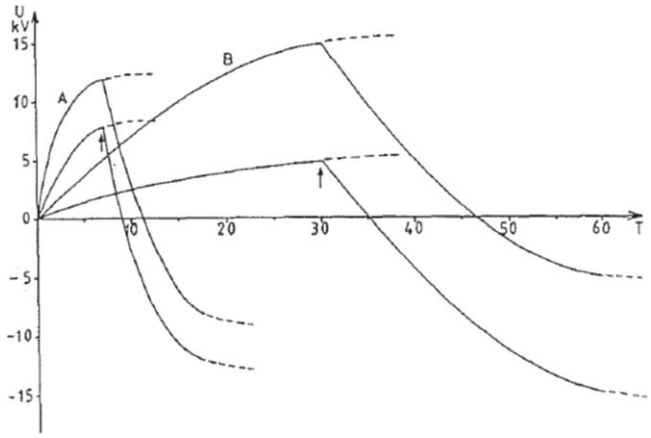

Figure 41. The time dependence of max and min voltages of the initial zero contour for the coated (A) and uncoated spacer (B). The time (T) is given in days. The arrows indicate polarity reversals. Figure reproduced with permission from CIGRE, [12], © 1986.

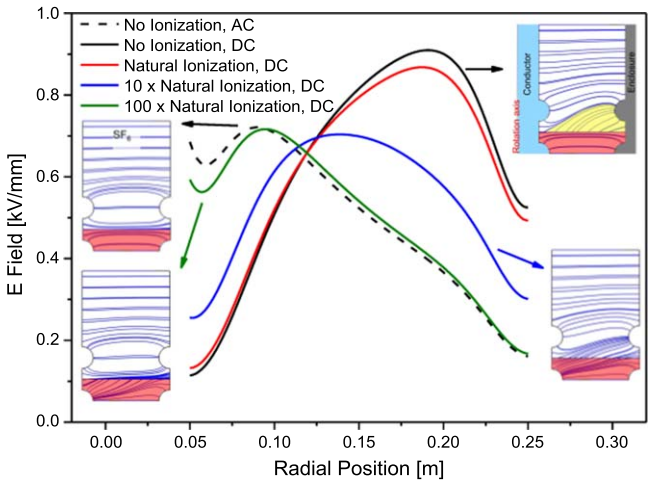

Figure 42. Electrical field at the solid–gas interface for various ion production rates. Insets show field lines in the gas (white) and solid (red) with example of ion capture volume (yellow region). Reproduced with permission from [99].

and conditions are selected to ensure replicability of tests to obtain the similar measured values. We recommend the conductivity measurement guidelines proposed in [102], by Salthouse. Based on this criterion, extension of measurement time to 24 h is needed to further ensure the stability and accuracy of the results. The measurement environment is suggested to be combined with the real operating environment of the insulator, especially for the use of nonlinear materials as modified insulators.

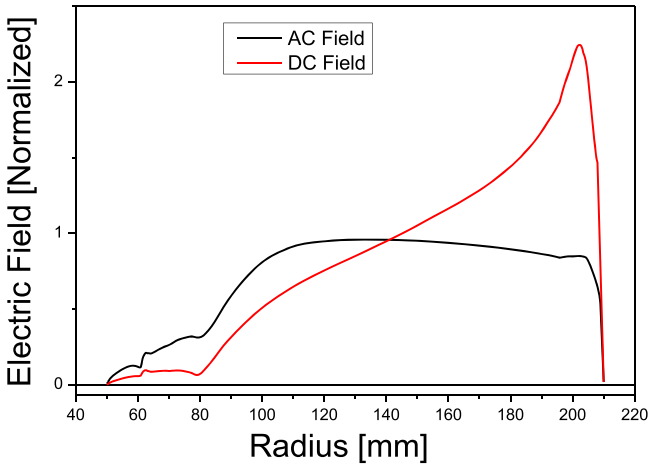

Figure 43. Comparison between capacitive and steady-state resistive electric field strength distribution (gas side) for the HVAC partition [11].

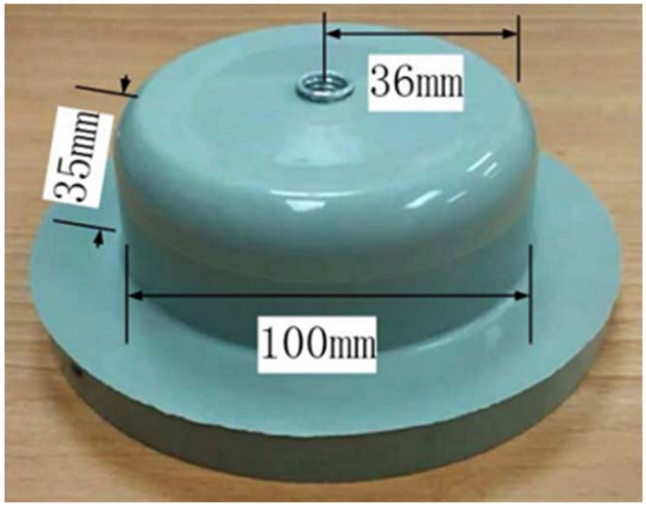

Figure 44. Side view of the charge adaptively controlling spacer. © 2018 IEEE. Reprinted, with permission, from [74].

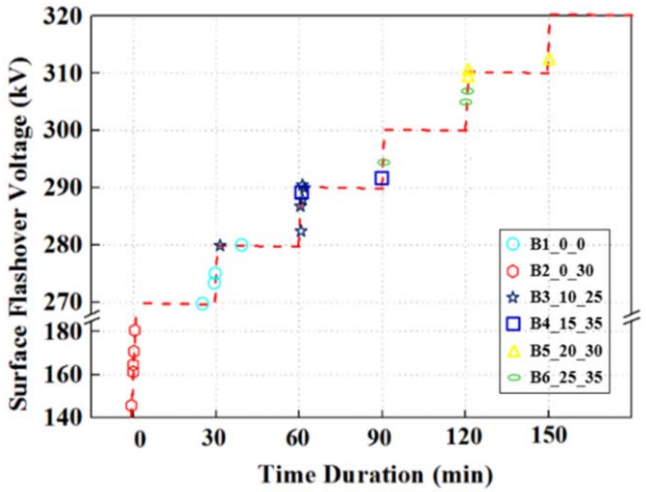

Figure 45. DC surface flashover test results of experimental samples (red line shows the increasing of dc voltage). © 2019 IEEE. Reprinted, with permission, from [76].

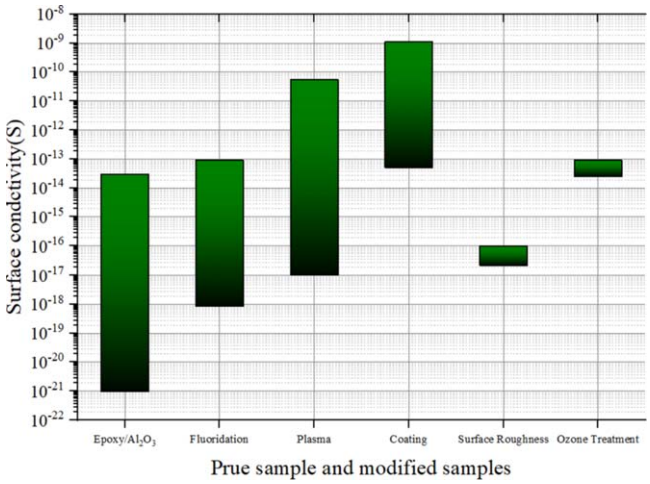

Figure 46. Distribution range of the surface conductivity of epoxy based samples before and after surface modification.

7.2. Conductivity and traps

Regarding the all charge tailoring techniques mentioned in this work, resistivity and traps are parameters that researchers concerned more about. The transition of electrons from the Fermi level to the conduction band requires energy to overcome the forbidden band whose width represents the resistivity of the polymer. When the polymer is modified either by surface modification or the volume doping, it is equivalent to introduce new impurities whose energy levels locates intermittently between the Fermi level and the conduction band of the polymer. Under such case, when the electrons cross the forbidden band, the energy levels introduced by impurities serves as a 'step', and it will be easier for electrons to overcome the forbidden band before reaching the conduction band. As a consequence, it can be conceived that the forbidden band becomes narrower and the trap density of the material becomes shallower, resulting in smaller resistivity [103].

As has been indicated by researchers that shallow traps increase surface charge decay, which is similar to the effect of increasing surface conductivity. Meanwhile, it has been verified that a surface with higher conductivity facilitates surface charge decay in a manner of surface leakage current while surface charge decays through bulk or/and recombination with charges of opposite polar in air when a surface with low conductivity s used [104–106]. It should be emphasized that deep traps can only be effective to inhibition of charge injection as a manner to suppress surface charge accumulation in case they are being created in the electrode/dielectric interface other than over the gas/solid interface-which prevents charge decay from insulator surface.

8. Conclusion

This paper introduces a Dam model, based on which surface charge tailoring techniques are classified and reviewed in a manner of increasing surface charge decay, inhibiting homopolar charges from volume conduction, decaying/avoiding

charges at high electric field, and initiatively controlling and decaying charges. Technical solutions of different charge tailoring methods are compared and discussed. The outlook of potential solutions to suppress charge accumulation is recommended and discussed based on industrial consideration. Based on the reviewing of published literature, we can sense that the current researches still needs further improvement, especially in the unity of measurement methods as well as the mechanism of increasing of surface flashover voltage. Meanwhile, for further studies, the transition from laboratory research to industrial production should also be considered. Before successfully developing of charge-free insulators, the progress and improvement in this field requires our joint efforts both in charge tailoring mechanism and treatment method.

Acknowledgments

This work was supported in part by the National Natural Science Foundation of China (Grant No. 51677113).

ORCID iDs

Geng Chen https://orcid.org/0000-0003-1357-1294
Zhipeng Lei https://orcid.org/0000-0002-8559-8501
Yang Cao https://orcid.org/0000-0001-7034-2792
Chuanyang Li https://orcid.org/0000-0002-3702-2647

References

[1] Li C, Lin C, Zhang B, Li Q, Liu W, Hu J and He J 2018 Understanding surface charge accumulation and surface flashover on spacers in compressed gas insulation *IEEE Trans. Dielectr. Electr. Insul.* **25** 1152–66
[2] Cooke C M 1982 Charging of insulator surfaces by ionization and transport in gases *IEEE Trans. Electr. Insul.* **EI-17** 172–8
[3] Zhang L *et al* 2020 Gas–solid interface charge characterization techniques for HVDC GIS/GIL insulators *High Voltage* **5** 95–109
[4] Dey A, De S, De A and De S K 2004 Characterization and dielectric properties of polyaniline-TiO_2 nanocomposites *Nanotechnology* **15** 1277–83
[5] Pan L K, Sun C Q, Chen T P, Li S, Li C M and Tay B K 2004 Dielectric suppression of nanosolid silicon *Nanotechnology* **15** 1802–6
[6] Tanaka T 2005 Dielectric nanocomposites with insulating properties *IEEE Trans. Dielectr. Electr. Insul.* **12** 914–28
[7] Wang T, Zhang B, Li D-Y, Hou Y-C and Zhang G-X 2020 Metal nanoparticle-doped epoxy resin to suppress surface charge accumulation on insulators under DC voltage *Nanotechnology* **31** 324001
[8] Wang T-Y, Zhang B-Y, Li D-Y, Hou Y-C and Zhang G-X 2020 A single-electron tunneling model: a theoretical analysis of a metal nanoparticle-doped epoxy resin to suppress surface charge accumulation on insulators subjected to DC voltages *Nanotechnology* **31** 475707
[9] Xue J, Chen J-H, Dong J-H, Deng J and Zhang G-J 2020 Enhancing flashover performance of alumina/epoxy spacers by adaptive surface charge regulation using graded conductivity coating *Nanotechnology* **31** 364002
[10] Guan H, Chen X, Du H, Jiang T, Paramane A and Zhou H 2020 Surface potential decay and DC surface flashover characteristics of DBD plasma-treated silicone rubber *Nanotechnology* **31** 424005
[11] Riechert U, Straumann U and Gremaud R 2016 Compact gas-insulated systems for high voltage direct current transmission: basic design *IEEE PES Transmission & Distribution Conf. & Exposition (T&D) (Dallas,TX, USA, 3-5 May 2016)* (Dallas, Texas, USA: Kay Bailey Hutchison Convention Center) pp 1–5
[12] Alvinsson R, Borg E, Hjortsberg A, Höglund T and Hörnfeldt S 1986 GIS for HVDC converter stations *CIGRE (International conference on large large high voltage electric systems, 1986)* 1–7
[13] Mendik M, Lowder S M and Elliott F 1999 Long term performance verification of high voltage DC GIS *IEEE Transmission and Distribution Conference* 2 (IEEE) pp 484–8 (https://ieeexplore.ieee.org/abstract/document/756101)
[14] Li C *et al* 2020 Charge cluster triggers unpredictable insulation surface flashover in pressurized SF6 *J. Phys. D: Appl. Phys.* **54** 015308
[15] Li C *et al* 2019 Surface charging phenomenon on HVDC spacers in compressed SF_6 insulation and charge tailoring strategies *J. Power Energy Syst.* **6** 83–99
[16] Li C, Lin C, Chen G, Tu Y, Zhou Y, Li Q, Zhang B and He J 2019 Field-dependent charging phenomenon of HVDC spacers based on dominant charge behaviors *Appl. Phys. Lett.* **114**
[17] Li C, Hu J, Lin C and He J 2017 The potentially neglected culprit of DC surface flashover: electron migration under temperature gradients *Sci. Rep.* **7**
[18] Götz T *et al* 2019 Progress on Partial discharge detection under DC voltage stress *Interim Report of WG* D1.63 CIGRE
[19] An Z, Yin Q, Liu Y, Zheng F, Lei Q and Zhang Y 2015 Modulation of surface electrical properties of epoxy resin insulator by changing fluorination temperature and time *IEEE Trans. Dielectr. Electr. Insul.* **22** 526–34
[20] Liu Y, An Z, Cang J, Zhang Y and Zheng F 2012 Significant suppression of surface charge accumulation on epoxy resin by direct fluorination *IEEE Trans. Dielectr. Electr. Insul.* **19** 1143–50
[21] Liu Y, An Z, Cang J, Zheng F and Zhang Y 2011 Preliminary study on surface properties of surface fluorinated epoxy resin insulation *IEEE Proc.2011 Int. Conf. on Electrical Insulating Materials (Kyoto, Japan, 6-10 Sept. 2011)* pp 109–12
[22] Liu Y, An Z, Yin Q, Zheng F, Lei Q and Zhang Y 2013 Characteristics and electrical properties of epoxy resin surface layers fluorinated at different temperatures *IEEE Trans. Dielectr. Electr. Insul.* **20** 1859–68
[23] Liu Y, An Z, Yin Q, Zheng F, Zhang Y and Lei Q 2013 Rapid potential decay on surface fluorinated epoxy resin samples *J. Appl. Phys.* **113** 164105
[24] Que L, An Z, Ma Y, Shan F, Zhang Y, Zheng F and Zhang Y 2018 High resistance of surface fluorinated epoxy insulators to surface discharge in SF_6 gas *IEEE Trans. Dielectr. Electr. Insul.* **25** 245–52
[25] Zhang B, Zhang G, Wang Q, Li C, Jinliang H and An Z 2015 Suppression of surface charge accumulation on Al_2O_3-filled epoxy resin insulator under DC voltage by direct fluorination *AIP Adv.* **5** 127207
[26] Mohamad A, Chen G, Zhang Y and An Z 2015 Surface fluorinated epoxy resin for high voltage DC application *IEEE Trans. Dielectr. Electr. Insul.* **22** 101–8

[27] Mohamad A, Chen G, Zhang Y and An Z 2016 Moisture effect on surface fluorinated epoxy resin for high-voltage DC applications *IEEE Trans. Dielectr. Electr. Insul.* **23** 1148–55

[28] Mohamad A, Chen G, Zhang Y and An Z 2013 Influence of fluorination time on surface flashover of polymeric insulation *IEEE Conf. on Electrical Insulation and Dielectric Phenomena (Shenzhen, China, 20-23 Oct. 2013)* pp 482–5 (https://ieeexplore.ieee.org/abstract/document/6748202)

[29] Mohamad A, Chen G, Zhang Y and An Z 2013 Surface potential decay measurements on fluorinated polymeric insulation for high voltage DC applications *IEEE Conf. on Electrical Insulation and Dielectric Phenomena (Shenzhen, China, 20-23 Oct. 2013)* pp 1132–5 (https://ieeexplore.ieee.org/abstract/document/6747065)

[30] Mohamad A, Chen G, Zhang Y and An Z 2014 Mechanisms for surface potential decay on fluorinated epoxy in high voltage DC applications *IEEE Conf. on Electrical Insulation and Dielectric Phenomena* pp 863–6

[31] Du B, Du Q, Li J and Liang H 2018 Carrier mobility and trap distribution dependent flashover characteristics of epoxy resin *IET Gener. Transmi. Distrib.* **12** 466–71

[32] Du B, Ran Z, Li J and Liang H 2019 Novel insulator with interfacial sigma-FGM for DC compact gaseous insulated pipeline *IEEE Trans. Dielectr. Electr. Insul.* **26** 818–25

[33] Li C, He J and Hu J 2016 Surface morphology and electrical characteristics of direct fluorinated epoxy-resin/alumina composite *IEEE Trans. Dielectr. Electr. Insul.* **23** 3071–7

[34] Li C, Hu J, Lin C and He J 2016 The control mechanism of surface traps on surface charge behavior in alumina-filled epoxy composites *J. Phys. D: Appl. Phys.* **49**

[35] Li C, Hu J, Lin C, Zhang B, Zhang G and He J 2016 Fluorine gas treatment improves surface degradation inhibiting property of alumina-filled epoxy composite *AIP Adv.* **6**

[36] Li C, Hu J, Lin C, Zhang B, Zhang G and He J 2017 Surface charge migration and DC surface flashover of surface-modified epoxy-based insulators *J. Phys. D: Appl. Phys.* **50**

[37] Que L, An Z, Ma Y, Xie D, Zheng F and Zhang Y 2017 Improved DC flashover performance of epoxy insulators in SF_6 gas by direct fluorination *IEEE Trans. Dielectr. Electr. Insul.* **24** 1153–61

[38] Shao T, Kong F, Lin H, Ma Y, Xie Q and Zhang C 2018 Correlation between surface charge and DC surface flashover of plasma treated epoxy resin *IEEE Trans. Dielectr. Electr. Insul.* **25** 1267–74

[39] Shao T, Liu F, Hai B, Ma Y, Wang R and Ren C 2017 Surface modification of epoxy using an atmospheric pressure dielectric barrier discharge to accelerate surface charge dissipation *IEEE Trans. Dielectr. Electr. Insul.* **24** 1557–65

[40] Wang R, Lin H, Gao Y, Ren C, Ostrikov K and Shao T 2017 Inorganic nanofilms for surface charge control on polymer surfaces by atmospheric-pressure plasma deposition *J. Appl. Phys.* **122** 233302

[41] Zhang C, Lin H, Zhang S, Xie Q, Ren C and Shao T 2017 Plasma surface treatment to improve surface charge accumulation and dissipation of epoxy resin exposed to DC and nanosecond-pulse voltages *J. Phys. D: Appl. Phys.* **50** 405203

[42] Zhang C, Ma Y, Kong F, Wang R, Ren C and Shao T 2019 Surface charge decay of epoxy resin treated by AP-DBD deposition and direct fluorination *IEEE Trans. Dielectr. Electr. Insul.* **26** 768–75

[43] Zhang C, Ma Y, Kong F, Yan P, Chang C and Shao T 2019 Atmospheric pressure plasmas and direct fluorination treatment of Al_2O_3-filled epoxy resin: a comparison of surface charge dissipation *Surf. Coat. Technol.* **362** 1–11

[44] Hai B, Zhang C, Wang R, Zhang S, Chen G and Shao T 2017 Plasma-deposited SiO_2-like thin film suppresses charge accumulation on epoxy resin surface *High Voltage Technol.* **43** 375–84 (in Chinese)

[45] Yue W, Min D, Nie Y and Li S 2018 Plasma treatment enhances surface flashover performance of EP/Al_2O_3micro-composite in vacuum *2018 12th Int. Conf. on the Properties and Applications of Dielectric Materials (ICPADM)* pp 1086–9

[46] Tu Y, Zhou F, Cheng Y, Jiang H, Wang C, Bai F and Lin J 2018 The control mechanism of micron and nano SiO_2/epoxy composite coating on surface charge in epoxy resin *IEEE Trans. Dielectr. Electr. Insul.* **25** 1275–84

[47] Tu Y, Zhou F, Jiang H, Bai F, Wang C, Lin J and Cheng Y 2018 Effect of nano-TiO_2/EP composite coating on dynamic characteristics of surface charge in epoxy resin *IEEE Trans. Dielectr. Electr. Insul.* **25** 1308–17

[48] Gao Y, Du B, Cui J and Wu K 2011 Effect of gamma-ray irradiation on lateral charge motion on surface of laminated polymer insulating materials *IEEE Annual Report Conf. on Electrical Insulation and Dielectric Phenomena, Vols 1 And 2* pp 153–6

[49] Gao Y, Du B, Ma Z and Zhu X 2010 Decay behavior of surface charge on gamma-ray irradiated epoxy resin *IEEE Proc. 2010 IEEE Int. Conf. on Solid Dielectrics* (https://doi.org/10.1109/ICSD.2010.5568073)

[50] Huang Y, Min D, Xie D, Li S, Wang X and Lin S 2017 Surface flashover performance of epoxy resin microcomposites infulenced by ozone treatment *2017 Int. Symp. on Electrical Insulating Materials*

[51] Baytekin H T, Baytekin B, Hermans T M, Kowalczyk B and Grzybowski B A 2013 Control of surface charges by radicals as a principle of antistatic polymers protecting electronic circuitry *Science* **341** 1368–71

[52] Li C, Hu J, Lin C and He J 2016 Hot electron injection regulation in Al_2O_3-filled epoxy resin composite using Cr_2O_3 coatings *IEEE Conf. on Electrical Insulation and Dielectric Phenomena* pp 101–4

[53] Zhang B, Gao W, Hou Y and Zhang G 2018 Surface charge accumulation and suppression on fullerene-filled epoxy-resin insulator under DC voltage *IEEE Trans. Dielectr. Electr. Insul.* **25** 2011–9

[54] He S, Lin C, Hu J, Li C and He J 2018 Tailoring charge transport in epoxy based composite under temperature gradient using $K_2Ti_6O_{13}$ and asbestine whiskers *J. Phys. D: Appl. Phys.* **51**

[55] Ootera H and Nakanishi K 1988 Analytical method for evaluating surface charge distribution on a dielectric from capacitive probe measurement-application to a cone-type spacer in +or-500 kV DC-GIS *IEEE Trans. Power Deliv.* **3** 165–72

[56] Nitta T and Nakanishi K 1991 Charge accumulation on insulating spacers for HVDC GIS *IEEE Trans. Electr. Insul.* **26** 418–27

[57] Fujinami H, Takuma T, Yashima M and Kawamoto T 1989 Mechanism and effect of DC charge accumulation on SF_6 gas insulated spacers *IEEE Power Eng. Rev.* **9** 62

[58] Cooke C M and Trump J G 1973 Post-type support spacers for compressed gas-insulated cables *IEEE Trans. Power Appar. Syst.* **PAS-92** 1441–7

[59] Nakanishi K, Yoshioka A, Arahata Y and Shibuya Y 1983 Surface charging on epoxy spacer At Dc stress in compressed SF_6 GAS *IEEE Trans. Power Appar. Syst.* **PAS-102** 3919–27

[60] Hasegawa T, Yamaji K, Hatano M, Endo F, Rokunohe T and Yamagiwa T 1997 Development of insulation structure and enhancement of insulation reliability of 500 kV DC GIS *IEEE Trans. Power Deliv.* **12** 194–202

[61] Volpov E 2004 Dielectric strength coordination and generalized spacer design rules for HVAC/DC SF_6 gas insulated systems *IEEE Trans. Dielectr. Electr. Insul.* **11** 949–63

[62] Tu Y, Chen G, Li C, Wang C, Ma G, Zhou H, Ai X and Cheng Y 2019 100 kV HVDC SF_6/N_2 gas-insulated transmission line *IEEE Trans. Power Deliv.* **35** 1

[63] Jia Z, Zhang Q, Zhang B, Fan J, Li J and Li P 2009 Flashover characteristics of insulators in SF_6 under DC *High Voltage Technol.* **35** 1903–7 (in Chinese)

[64] Liang H, Du B, Li J, Li Z and Li A 2018 Effects of non-linear conductivity on charge trapping and de-trapping behaviours in epoxy/SiC composites under DC stress *IET Sci. Meas. Technol.* **12** 83–9

[65] Li J, Liang H, Du B and Wang Z 2019 Surface functional graded spacer for compact HVDC gaseous insulated system *IEEE Trans. Dielectr. Electr. Insul.* **26** 664–7

[66] Du B, Liang H, Li J and Zhang C 2018 Temperature dependent surface potential decay and flashover characteristics of epoxy/SiC composites *IEEE Trans. Dielectr. Electr. Insul.* **25** 631–8

[67] He S, Li C, Lin C, Hu J, He J and Sun Z 2019 Feasibility analysis and verification of potential application of nonlinear materials in charge control of gas–solid interface *J. Power Syst. Autom.* **32** 1–7 (in Chinese)

[68] Du B, Liang H and Li J 2019 Interfacial E-field self-regulating insulator considered for DC GIL application *IEEE Trans. Dielectr. Electr. Insul.* **26** 801–9

[69] Xue J, Chen J, Dong J, Sun G, Deng J and Zhang G-J 2020 A novel sight for understanding surface charging phenomena on downsized HVDC GIL spacers with non-uniform conductivity *Int. J. Electr. Power Energy Syst.* **120** 105979

[70] Xue J, Chen J, Dong J, Wang H, Li W, Deng J and Zhang G 2019 The regulation mechanism of SiC/epoxy coatings on surface charge behavior and flashover performance of epoxy/alumina spacers *J. Phys. D: Appl. Phys.* **52** 405502

[71] Xue J, Li Y, Dong J, Chen J, Li W, Deng J and Zhang G 2020 Surface charge transport behavior and flashover mechanism on alumina/epoxy spacers coated by SiC/epoxy composites with varied SiC particle size *J. Phys. D: Appl. Phys.* **53** 155503

[72] Pan Z, Tang J, Pan C, Luo Y, Liu Q and He H 2020 Contribution of nano-SiC/epoxy coating with nonlinear conduction characteristic to surface charge accumulation under DC voltage *J. Phys. D: Appl. Phys.* **53** 365303

[73] Li C, Lin C, Hu J, Liu W, Li Q, Zhang B, He S, Yang Y, Liu F and He J 2018 Novel HVDC spacers by adaptively controlling surface charges: I. Charge transport and control strategy *IEEE Trans. Dielectr. Electr. Insul.* **25** 1238–47

[74] Li C, Lin C, Yang Y, Zhang B, Liu W, Li Q, Hu J, He S, Liu X and He J 2018 Novel HVDC spacers by adaptively controlling surface charges: II. Experiment *IEEE Trans. Dielectr. Electr. Insul.* **25** 1248–58

[75] Li C, Lin C, Zhang B, Liu W, Yang Y, Liu F, Liu X, Hu J and He J 2018 Novel HVDC spacers by adaptively controlling surface charges: III. Industrialization prospects *IEEE Trans. Dielectr. Electr. Insul.* **25** 1259–66

[76] Li C, Liu B, Wang J, Gong R, Wang G, Lei Z, Fabiani D, Lin C and Hu J 2019 Novel HVDC spacers in GIS/GIL by adaptively controlling surface charges—insulation compounding scheme *2019 2nd Int. Conf. on High Voltage Engineering and Power Systems (ICHVEPS)* pp 268–71

[77] Zhang G, Wang X, Yan Z, Liu Y, Okada M, Yasuoka K and Ishii S 2002 Optical studies of surface discharge under dc voltage in vacuum *IEEE Trans. Dielectr. Electr. Insul.* **9** 187–93

[78] Griseri V, Dissado L A, Fothergill J, Teyssedre G and Laurent C 2002 Electroluminescence excitation mechanisms in an epoxy resin under divergent and uniform field *IEEE Trans. Dielectr. Electr. Insul.* **9** 150–60

[79] Lin C *et al* 2020 Luminescence reveals micro discharge as a potential triggering factor for surface flashover *Journal of Physics D: Applied Physics* **53** 445103

[80] Shao T, Wang R, Zhang C and Yan P 2018 Atmospheric-pressure pulsed discharges and plasmas: mechanism, characteristics and applications *High Voltage* **3** 14–20

[81] Shao T, Yang W, Zhang C, Niu Z, Yan P and Schamiloglu E 2014 Enhanced surface flashover strength in vacuum of polymethylmethacrylate by surface modification using atmospheric-pressure dielectric barrier discharge *Appl. Phys. Lett.* **105** 071607

[82] Du B, Liang H and Li J 2019 Surface coating affecting charge distribution and flashover voltage of cone-type insulator under DC stress *IEEE Trans. Dielectr. Electr. Insul.* **26** 714–21

[83] Zhang B, Wang Q, Zhang Y, Gao W, Hou Y and Zhang G 2019 A self-assembled, nacre-mimetic, nano-laminar structure as a superior charge dissipation coating on insulators for HVDC gas-insulated systems *Nanoscale* **11** 18046–51

[84] Iwabuchi H, Donen T, Matsuoka S, Kumada A, Hidaka K, Hoshina Y and Takei M 2012 Influence of surface-conductivity nonuniformity on charge accumulation of GIS downsized model spacer under DC field application *Electr. Eng. Japan* **181** 29–36

[85] Xue J, Wang H, Chen J, Li K, Liu Y, Song B, Deng J and Zhang G 2018 Effects of surface roughness on surface charge accumulation characteristics and surface flashover performance of alumina-filled epoxy resin spacers *J. Appl. Phys.* **124** 083302

[86] Chu P, Zhang H, Zhao J, Gao F, Guo Y, Dang B and Zhang Z 2017 On the volume resistivity of silica nanoparticle filled epoxy with different surface modifications *Composites* A **99** 139–48

[87] Hanna R, Lesaint O and Zavattoni L 2016 Dark current measurements in humid SF_6 at high uniform electric field *IEEE Conf. on Electrical Insulation and Dielectric Phenomena* pp 19–22

[88] Zavattoni L, Hanna R, Lesaint O and Gallot-Lavallee O 2015 Dark current measurements in humid SF_6: influence of electrode roughness, relative humidity and pressure *J. Phys. D: Appl. Phys.* **48** 375501

[89] Zavattoni L, Lesaint O and Gallot-Lavallee O 2013 Dark current measurements in pressurized Air, N_2, and SF_6 *IEEE Conf. on Electrical Insulation and Dielectric Phenomena* pp 659–62

[90] Messerer F and Boeck W 1999 High resistance surface coating of solid insulating components for HVDC metal enclosed equipment *1999 11th Int. Symp. on High Voltage Engineering* 4, pp 63–6

[91] Messerer F, Finkel M and Boeck W 2002 Surface charge accumulation on HVDC-GIS-spacer *Conf. Record of the the 2002 IEEE Int. Symp. on Electrical Insulation (Cat. No.02CH37316)* pp 421–5

[92] Winter A, Kindersberger J, Tenzer M, Hinrichsen V, Zavattoni L, Lesaint O, Muhr M and Imamovic D 2015 Solid/gaseous insulation systems for compact HVDC solutions *Cigre Sci. Eng.* **1** 13

[93] Winter A, Kindersberger J, Hinrichsen V, Imamovic D and Tenzer M 2013 Compact gas–solid insulating systems for high-field-stress in HVDC applications *CIGRE Study Committee B3 & Study Committee D1 Coll.*

[94] Zhang B and Zhang G 2018 A summary of the research on the charge characteristics of the solid–gas interface in DC GIL: II. Charge regulation and suppression strategies *J. Electr. Eng.* **33** 5145–58 (in Chinese)

[95] Mangelsdorf C W and Cooke C M 1978 Static charge accumulated by epoxy post insulation stressed at high DC voltages *Conf. on Electrical Insulation & Dielectric Phenomena—Annual Report 1978* pp 220–7

[96] Giboulet E F A *et al* 2012 Gas insulated systems for HVDC: DC stress at DC and AC systems *CIGRÉ Brochure* CIGRÉ Working Group D1.03 (TF11)

[97] Riechert U, Hama H, Endo F, Juhre K, Kindersberger J, Meijer S, Neumann C, Okabe S and Schichler U 2010 On behalf of CIGRÉ task force D1.03.11. 2010 gas insulated systems for HVDC *2010 ETG Fachtagung: Isoliersysteme bei Gleich- und Mischfeldbeanspruchung (Köln, Germany)*

[98] Straumann U, Schueller M and Franck C 2012 Theoretical investigation of HVDC disc spacer charging in SF_6 gas insulated systems *IEEE Trans. Dielectr. Electr. Insul.* **19** 2196–205

[99] Gremaud R, Molitor F, Doiron C, Krivda A, Christen T, Johansson K, Lavesson N, Riechert U and Straumann U 2013 Solid–gas interfaces in DC gas insulated systems *Grenzflächen in elektrischen Isoliersystemen - Beiträge der 4. ETG-Fachtagung (Dresden, Germany)*

[100] Gremaud R *et al* 2016 Solid–gas insulation in HVDC gas-insulated system: Measurement, modeling and experimental validation for reliable operation *CIGRÉ Report D1-101, 46th CIGRÉ Session (Palais des Congrès de Paris, Paris, France)*

[101] Riechert U, Straumann U, Gremaud R and Callavik M 2016 Compact gas-insulated systems for high voltage direct current transmission: design and testing *2016 IEEE PES Transmission & Distribution Conf. & Exposition (T&D)* (Dallas, Texas, USA: Kay Bailey Hutchison Convention Center) pp 1–5

[102] Salthouse E C and McIlhagger D S 1962 The measurement of surface resistivity *Proc. IEE-Part A: Power Engineering* pp 41–4

[103] Zhao W, Zhang G and Yan Z 2007 Influence of trap parameters of composite materials on its flashover characteristics under high voltage pulses in vacuum *Chin. Soc. Electr. Eng.* 11–7 (in Chinese)

[104] Winter A and Kindersberger J 2012 Stationary resistive field distribution along epoxy resin insulators in air under DC voltage *IEEE Trans. Dielectr. Electr. Insul.* **19** 1732–9

[105] Kindersberger J and Lederle C 2008 Surface charge decay on insulators in air and sulfurhexafluorid: I. Simulation *IEEE Trans. Dielectr. Electr. Insul.* **15** 941–8

[106] Kindersberger J and Lederle C 2008 Surface charge decay on insulators in air and sulfurhexafluorid: II. Measurements *IEEE Trans. Dielectr. Electr. Insul.* **15** 949–57